

# RECLAMATION

*Managing Water in the West*

Hydraulic Laboratory Report HL-2015-03

## **Cle Elum Dam Intake Structure Design for Downstream Fish Passage**



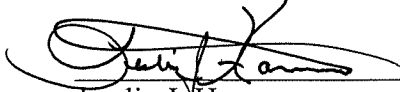
**U.S. Department of the Interior  
Bureau of Reclamation  
Technical Service Center  
Hydraulic Investigations and Laboratory Services Group  
Denver, Colorado**

November 2016

REPORT DOCUMENTATION PAGE			Form Approved OMB No. 0704-0188		
<p>The public reporting burden for this collection of information is estimated to average 1 hour per response, including the time for reviewing instructions, searching existing data sources, gathering and maintaining the data needed, and completing and reviewing the collection of information. Send comments regarding this burden estimate or any other aspect of this collection of information, including suggestions for reducing the burden, to Department of Defense, Washington Headquarters Services, Directorate for Information Operations and Reports (0704-0188), 1215 Jefferson Davis Highway, Suite 1204, Arlington, VA 22202-4302. Respondents should be aware that notwithstanding any other provision of law, no person shall be subject to any penalty for failing to comply with a collection of information if it does not display a currently valid OMB control number.</p> <p><b>PLEASE DO NOT RETURN YOUR FORM TO THE ABOVE ADDRESS.</b></p>					
1. REPORT DATE (DD-MM-YYYY) 11-13-2015		2. REPORT TYPE Technical		3. DATES COVERED (From - To) May 2013 – Jan 2015	
4. TITLE AND SUBTITLE  Cle Elum Dam Intake Structure Design for Downstream Fish Passage			5a. CONTRACT NUMBER		
			5b. GRANT NUMBER		
			5c. PROGRAM ELEMENT NUMBER		
6. AUTHOR(S) Leslie J. Hanna Jim Higgs			5d. PROJECT NUMBER		
			5e. TASK NUMBER		
			5f. WORK UNIT NUMBER		
7. PERFORMING ORGANIZATION NAME(S) AND ADDRESS(ES) U.S. Dept. of the Interior, Bureau of Reclamation Technical Service Center, 86-68560 Denver, CO 80225			8. PERFORMING ORGANIZATION REPORT NUMBER  HL-2012-01		
9. SPONSORING/MONITORING AGENCY NAME(S) AND ADDRESS(ES) U.S. Department of the Interior, Bureau of Reclamation Research and Development Office, 86-69000 P.O. Box 25007 Denver, CO 80225			10. SPONSOR/MONITOR'S ACRONYM(S)		
			11. SPONSOR/MONITOR'S REPORT NUMBER(S)		
12. DISTRIBUTION/AVAILABILITY STATEMENT National Technical Information Service, 5285 Port Royal Road, Springfield, VA 22161 <a href="http://www.ntis.gov">http://www.ntis.gov</a>					
13. SUPPLEMENTARY NOTES					
14. ABSTRACT Reclamation's Hydraulics Laboratory in Denver, Colorado conducted physical hydraulic model studies to support design of the intake for a proposed downstream fish passage system at Cle Elum Dam. This report addresses only the development of the intake and the components that help the flow to transition into the fish passage channel. The purpose of this study was to determine transition geometries that would provide optimal hydraulic conditions for continuous safe downstream juvenile fish passage. Both numerical and physical modeling were used to develop and refine the final design.					
15. SUBJECT TERMS intake, inlet, downstream fish passage, hydraulic model, high head dam, storage reservoir fish passage					
16. SECURITY CLASSIFICATION OF:			17. LIMITATION OF ABSTRACT	18. NUMBER OF PAGES	19a. NAME OF RESPONSIBLE PERSON
REPORT	ABSTRACT	THIS PAGE	SAR	95	Robert F. Einhellig
UU	UU	UU			19b. TELEPHONE NUMBER (Include area code) 303-445-2142

# Cle Elum Dam Intake Structure Design for Downstream Passage

**Prepared by:**



Leslie J. Hanna

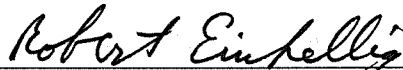
Hydraulic Engineer, Hydraulic Investigations and Laboratory Services Group, 86-68460



Jim Higgs

Hydraulic Engineer, Hydraulic Investigations and Laboratory Services Group, 86-68460

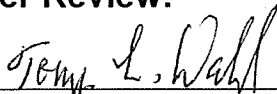
**Technical Approval:**



Robert Einhellig, P.E., Group Manager

Hydraulic Investigations and Laboratory Services Group, 86-68460

**Peer Review:**



Tony L. Wahl, P.E.

Hydraulic Engineer, Hydraulic Investigations and Laboratory Services Group, 86-68460

11/3/2016

Date



## **Mission Statements**

The mission of the Department of the Interior is to protect and provide access to our Nation's natural and cultural heritage and honor our trust responsibilities to Indian Tribes and our commitments to island communities.

---

The mission of the Bureau of Reclamation is to manage, develop, and protect water and related resources in an environmentally and economically sound manner in the interest of the American public.

## **Acknowledgments**

The State of Washington and Reclamation's Columbia Cascades Area Office funded this project. The authors thank the Yakima Storage Dams Fish Passage Core Team (Core team) for providing invaluable expert guidance on this project. Special thanks are due to the Hydraulics Laboratory shop staff who constructed the physical hydraulic models: Dane Cheek, Marty Poos, Jimmy Hastings and Jason Black.

## **Hydraulic Laboratory Reports**

The Hydraulic Laboratory Report series is produced by the Bureau of Reclamation's Hydraulic Investigations and Laboratory Services Group (Mail Code 86-68560), PO Box 25007, Denver, Colorado 80225-0007. See [http://www.usbr.gov/tsc/techreferences/hydraulics\\_lab/pubs/index.cfm](http://www.usbr.gov/tsc/techreferences/hydraulics_lab/pubs/index.cfm) for online publications.

## **Disclaimer**

The information provided in this report is believed to be appropriate and accurate for the specific purposes described herein, but users bear all responsibility for exercising sound engineering judgment in its application, especially to situations different from those studied. References to commercial products do not imply endorsement by the Bureau of Reclamation and may not be used for advertising or promotional purposes.

# CONTENTS

EXECUTIVE SUMMARY .....	1
BACKGROUND .....	3
INTRODUCTION .....	4
MODEL STUDY OVERVIEW .....	7
Operation Criteria .....	7
CFD modeling methods .....	11
Physical modeling methods .....	11
PRELIMINARY INLET STRUCTURE STUDIES .....	12
Interim flume CFD modeling .....	13
Interim flume physical modeling .....	21
Weir and ramp-weir tests .....	25
FINAL INLET CONFIGURATION .....	25
Attraction water velocities within the reservoir .....	31
Velocity gradients within the intake structure .....	33
Flow conditions downstream of the ramp-weir .....	35
Transition into the helix structure .....	39
CONCLUSIONS.....	40
REFERENCES .....	42
APPENDIX A – DESCRIPTION OF CFD MODELING.....	43
FLOW-3D.....	43
Simulation Assumptions .....	43
Solids model development.....	44
APPENDIX B .....	45
Inlet Transitions – Velocity Gradient Criteria 1.0 ft/s/ft .....	45
APPENDIX C .....	58
Weir and Ramp-Weir Tests .....	58
Vertical Weir Tests .....	59
Ramp-Weir Tests .....	66

# FIGURES

Figure 1. — Cle Elum Dam and spillway.....	5
Figure 2. — Location map of Cle Elum Dam.....	6
Figure 3. — Layout of proposed intake structure, helix and tunnel through right abutment. ....	7
Figure 4. — Intake structure concept with six separate inlets controlling flow into the helix. ....	9
Figure 5. — Looking down on the interim flume near the top of the spillway at Cle Elum Dam. ....	9
Figure 6. — Stoplog bays used to control flow into the interim flume. Operators have observed the best fish attraction when the flow is only through the center bay.....	10
Figure 7. — View from the deck above the stoplog structures looking at the upstream side of the Obermeyer gate at interim flume entrance. The gate is downstream from the stoplog bay (located under the deck at the bottom of the image).....	10
Figure 8. — Flow discharging from the interim flume into the stilling basin.....	11
Figure 9. — CFD model representing flow through center stoplog bay for the interim flume....	14
Figure 10. — Flow profile at centerline of center stoplog bay at 264 ft <sup>3</sup> /s with no stoplogs installed. The Obermeyer gate downstream of the stoplog slot is in the down position, and does not affect flow conditions. ....	14
Figure 11. — Flow profile at centerline of center stoplog bay at 308 ft <sup>3</sup> /s with stoplogs installed to a height of 2 ft. Reservoir water surface elevation is 4 ft above the weir crest. The Obermeyer gate downstream of the stoplog does not affect approach conditions and was not modeled.....	15
Figure 12. — Flow profile at centerline of center stoplog bay at 320 ft <sup>3</sup> /s with stoplogs installed to a height of 4 ft. Reservoir water surface elevation is 4 ft above the weir crest. The Obermeyer gate downstream of the stoplog does not affect approach conditions and was not modeled.....	15
Figure 13. — Flow profile at centerline of center stoplog bay at 324 ft <sup>3</sup> /s with stoplogs installed to a height of 6 ft. Reservoir water surface elevation is 4 ft above the weir crest. The Obermeyer gate downstream of the stoplog does not affect approach conditions and was not modeled.....	16
Figure 14. — Velocity and velocity gradient determined from the CFD model at 2 ft below water surface along the centerline of the center stoplog bay with no stoplogs installed. Discharge into flume is 264 ft <sup>3</sup> /s.....	17
Figure 15. — CFD velocity and velocity gradient 2 ft below water surface along the centerline of the center stoplog bay with stoplogs installed to a 2 ft height. Discharge into flume is 308 ft <sup>3</sup> /s. ....	18
Figure 16. — CFD velocity and velocity gradient 2 ft below water surface along the centerline of the center stoplog bay with stoplogs installed to a 4 ft height. Discharge into flume is 320 ft <sup>3</sup> /s. ....	19
Figure 17. — CFD velocity and velocity gradient 2 ft below water surface along the centerline of the center stoplog bay with stoplogs installed to a 6 ft height. Discharge into flume is 324 ft <sup>3</sup> /s. ....	20
Figure 18. — Physical model of the interim flume with a 4-ft high vertical weir spanning a width of 11 ft.....	22
Figure 19. — Comparison of physical (pink) and numerical modeling (blue) data for velocities measured 2 ft below the water surface at the bay centerline for 320 ft <sup>3</sup> /s. ....	23

Figure 20. — Comparison of physical and numerical modeling data for velocity gradients measured 2 ft below the water surface at the bay centerline for 320 ft <sup>3</sup> /s. ....	24
Figure 21. — Final design juvenile fish passage structure overview. ....	26
Figure 22. — Six inlets for the juvenile fish passage structure. Trash racks and metal gratings are not shown. ....	27
Figure 23. — Typical juvenile fish passage inlet. ....	27
Figure 24. — Profile view of the juvenile fish passage inlets and helix structures. ....	28
Figure 25. — Comparison of velocity gradients in the physical model with (pink) and without (green) an upstream ramp attached to the weir, using a weir height of 2.375 ft at 200 ft <sup>3</sup> /s. ....	29
Figure 26. — Overview of simulation with stereolithography (top) and without stereolithography (bottom). Critical features investigated from this design are labeled on the bottom image: ❶ attraction water velocities within the reservoir, ❷ velocity gradients within the intake structure, ❸ flow conditions downstream of the ramp-weir, and ❹ the transition into the helix structure. ....	31
Figure 27. — Depth averaged velocities for the Gate-down simulation. X values represent project stationing. ....	32
Figure 28. — Depth averaged velocities for the Gate-up simulation. ....	33
Figure 29. — Velocities for the gate-down simulation. The next-downstream inlet was modeled as a solid object (not containing an opening). ....	34
Figure 30. — Velocity and velocity gradient for the gate-down simulation. ....	34
Figure 31. — Velocities for the Gate-up simulation. The trashrack and grate support structures circled in red interfere with calculation of velocity gradients in the plane that is 2 feet below the reservoir water surface, causing disruption of the flow field. The downstream inlet was modeled as a solid object (not containing an opening). ....	35
Figure 32. — Velocity and velocity gradient for the gate-up simulation. The capture velocity of 8 ft/s was achieved slightly upstream of the gate peak (lines appear to overlap). The elevation for data extraction for the gate-up simulation crossed through the trashrack and grate support structure (Figure 31), causing the velocity output to be zero, and the velocity gradient computation used that value. ....	35
Figure 33. — Velocity magnitude, flow depth, and Froude number for the gate-down simulation. The gate object is shown in grey (very thin in the down position) and is arched. Once supercritical flow ( $Fr > 1$ ) is achieved, the flow remains supercritical indicating a hydraulic jump will not form. Standing waves were minor, less than 1 ft high. ....	37
Figure 34. — Velocity magnitude, flow depth, and Froude number for the gate-up simulation. The gate object is shown in grey. Once supercritical flow ( $Fr > 1$ ) is achieved, the flow remains supercritical indicating a hydraulic jump will not form. Due to this portion of the intake being submerged at this reservoir water surface elevation (ft) as shown in Figure 28 and Figure 31, the depth and Froude number computation is not correct for the range indicated in red. Standing waves were minor, less than 1 ft high. ....	38
Figure 35. — Velocity and depth for the gate-down simulation. ....	39
Figure 36. — Velocity and depth for the gate-up simulation. ....	40
Figure 37. — Schematic of final configuration for inlet gate, utilizing an Obermeyer gate to provide an adjustable ramp-weir height. The Obermeyer gate has an attached downstream ramp to maintain supercritical flow. ....	41

## APPENDIX FIGURES

Figure B-1. — Initial concept for intake structure design following bank line.....	46
Figure B-2. — Pinch valve used to control flow into initial intake structure design. ....	46
Figure B-3. — Initial design concept for individual inlets for intake structure.....	46
Figure B-4. — Centerline profile view for initial design of individual inlets for intake structure	47
Figure B-5. — Only three of the six inlets are used to represent the intake structure in the physical model. Adjacent reservoir topography was not included for the initial model runs. .....	48
Figure B-6. — Average velocities approaching the inlet for a flow rate of 400 ft <sup>3</sup> /s, measured 2 ft below the water surface at the inlet centerline. See figure B-3 for “End of sill” location.	49
Figure B-7. — Standing waves and turbulence at inlet show undesirable entrance conditions. ..	49
Figure B-8. — Inlet is modified into the T3 transition. ....	51
Figure B-9. — Transition T3 inlet operating at 400 ft <sup>3</sup> /s with an inlet sill depth of 3.5 ft. ....	51
Figure B-10. — Average velocities measured approaching and within the T3 transition inlet while operating at 400 ft <sup>3</sup> /s with a sill depth of 3.5 ft.....	52
Figure B-11. — Velocity gradient measured approaching and within the T3 transition inlet while operating at 400 ft <sup>3</sup> /s with a sill depth of 3.5 ft.....	52
Figure B-12. — T3 transition inlet operating at 200 ft <sup>3</sup> /s with a sill depth of 1.98 ft.....	53
Figure B-13. — Average velocities measured approaching and within the T3 transition inlet while operating at 200 ft <sup>3</sup> /s with a sill depth of 1.98 ft.....	53
Figure B-14. — Velocity gradient measured approaching and within the T3 transition inlet while operating at 200 ft <sup>3</sup> /s with a sill depth of 1.98 ft.....	54
Figure B-15. — T3 transition inlet operating at 400 ft <sup>3</sup> /s with a sill depth of 5.54 ft.....	54
Figure B-16. — T3 transition inlet operating at 200 ft <sup>3</sup> /s with a sill depth of 2.62 ft.....	55
Figure B-17. — Average velocities measured approaching and within the T3 transition inlet while operating at 400 ft <sup>3</sup> /s with a sill depth of 5.54 ft.....	55
Figure B-18. — Velocity gradient measured approaching and within the T3 transition inlet while operating at 400 ft <sup>3</sup> /s with a sill depth of 5.54 ft.....	56
Figure B-19. — Average velocities measured approaching and within the T3 transition inlet while operating at 200 ft <sup>3</sup> /s with a sill depth of 2.62 ft.....	56
Figure B-20. — Velocity gradient measured approaching and within the T3 transition inlet while operating at 200 ft <sup>3</sup> /s with a sill depth of 2.62 ft.....	57
Figure C-1. — The same flow with (left) and without (right) control valve throttling to provide cushioned drop. Flow at 200 ft <sup>3</sup> /s over 2.375 ft high ramp weir (Test Case #10). The throttling effect can be used for any weir or ramp-weir configuration. ....	59
Figure C-2. — Vertical weir height 5.5 ft operating at 400 ft <sup>3</sup> /s (left) and 200 ft <sup>3</sup> /s (right) with depth over the weir at 3.86 ft and 2.47 ft respectively.....	60
Figure C-3. — Vertical weir height 2.375 ft operating at 400 ft <sup>3</sup> /s (left) and 200 ft <sup>3</sup> /s (right) with depth over the weir at 3.96 ft and 2.37 ft respectively.....	60
Figure C-4. — Weir height 0.0 ft operating at 400 ft <sup>3</sup> /s (left) and 200 ft <sup>3</sup> /s (right) with depth over the weir or inlet sill at 4.45 ft and 2.87 ft respectively. ....	60

Figure C-5. — Average velocity measured 2 ft below the water surface approaching the 5.5 ft weir, operating at 400 ft <sup>3</sup> /s with a weir depth of 3.86 ft. ....	61
Figure C-6. — Velocity gradient measured 2 ft below the water surface approaching the 5.5 ft weir, operating at 400 ft <sup>3</sup> /s with a weir depth of 3.86 ft. ....	61
Figure C-7. — Average velocity measured 2 ft below the water surface approaching the 5.5 ft weir, operating at 200 ft <sup>3</sup> /s with a weir depth of 2.47 ft. ....	62
Figure C-8. — Velocity gradient measured 2 ft below the water surface approaching the 5.5 ft weir, operating at 200 ft <sup>3</sup> /s with a weir depth of 2.47 ft. ....	62
Figure C-9. — Average velocity measured 2 ft below the water surface approaching the 2.375 ft weir, operating at 400 ft <sup>3</sup> /s with a weir depth of 3.96 ft. ....	63
Figure C-10. — Velocity gradient measured 2 ft below the water surface approaching the 2.375 ft weir, operating at 400 ft <sup>3</sup> /s with a weir depth of 3.96 ft. ....	63
Figure C-11. — Average velocity measured 2 ft below the water surface approaching the 2.375 ft weir, operating at 200 ft <sup>3</sup> /s with a weir depth of 2.37 ft. ....	64
Figure C-12. — Velocity gradient measured 2 ft below the water surface approaching the 2.375 ft weir, operating at 200 ft <sup>3</sup> /s with a weir depth of 2.37 ft. ....	64
Figure C-13. — Average velocity measured 2 ft below the water surface approaching the 0.0 ft weir, operating at 400 ft <sup>3</sup> /s with a weir depth of 4.45 ft. ....	65
Figure C-14. — Velocity gradient measured 2 ft below the water surface approaching the 0.0 ft weir, operating at 400 ft <sup>3</sup> /s with a weir depth of 4.45 ft. ....	65
Figure C-15. — Average velocity measured 2 ft below the water surface approaching the 0.0 ft weir, operating at 200 ft <sup>3</sup> /s with a weir depth of 2.87 ft. ....	66
Figure C-16. — Velocity gradient measured 2 ft below the water surface approaching the 0.0 ft weir, operating at 200 ft <sup>3</sup> /s with a weir depth of 2.87 ft. ....	66
Figure C-17. — Ramp-weir height 5.5 ft operating at 400 ft <sup>3</sup> /s (left) and 200 ft <sup>3</sup> /s (right) with depth over the crest at 3.91 ft and 2.42 ft respectively ....	67
Figure C-18. — Ramp-weir height 2.375 ft operating at 400 ft <sup>3</sup> /s (left) and 200 ft <sup>3</sup> /s (right) with depth over the crest at 4.05 ft and 2.57 ft respectively. ....	67
Figure C-19. — Average velocity measured 2 ft below the water surface approaching the 5.5 ft ramp-weir, operating at 400 ft <sup>3</sup> /s with a crest depth of 3.91 ft. ....	68
Figure C-20. — Velocity gradient measured 2 ft below the water surface approaching the 5.5 ft ramp-weir, operating at 400 ft <sup>3</sup> /s with a crest depth of 3.91 ft. ....	68
Figure C-21. — Average velocity measured 2 ft below the water surface approaching the 5.5 ft ramp-weir, operating at 200 ft <sup>3</sup> /s with a crest depth of 2.42 ft. ....	69
Figure C-22. — Velocity gradient measured 2 ft below the water surface approaching the 5.5 ft ramp-weir, operating at 200 ft <sup>3</sup> /s with a crest depth of 2.42 ft. ....	69
Figure C-23. — Average velocity measured 2 ft below the water surface approaching the 2.375 ft ramp-weir, operating at 400 ft <sup>3</sup> /s with a crest depth of 4.05 ft. ....	70
Figure C-24. — Velocity gradient measured 2 ft below the water surface approaching the 2.375 ft ramp-weir, operating at 400 ft <sup>3</sup> /s with a crest depth of 4.05 ft. ....	70
Figure C-25. — Average velocity measured 2 ft below the water surface approaching the 2.375 ft ramp-weir, operating at 200 ft <sup>3</sup> /s with a crest depth of 2.57 ft. ....	71
Figure C-26. — Velocity gradient measured 2 ft below the water surface approaching the 2.375 ft ramp-weir, operating at 200 ft <sup>3</sup> /s with a crest depth of 2.57 ft. ....	71



# Executive Summary

The U.S. Bureau of Reclamation (Reclamation) is actively pursuing the development and construction of a downstream fish passage system at Cle Elum Dam. The system consists of a series of structures that will allow fish (primarily juvenile sockeye salmon, *Oncorhynchus nerka*) to self-guide into a structure that carries them around the dam and into the downstream river channel. This design includes an intake structure, helical fish passage channel (the helix), tunnel, and outfall.

Reclamation's Hydraulics Laboratory in Denver, Colorado conducted numerical and physical hydraulic model studies to support development of the fish passage system design. The intake structure that withdraws water and fish from the reservoir and leads to the helix is an important component that must attract fish to the passage system and safely draw them in with a gradually accelerating flow field that creates a velocity trap that fish cannot escape from. This report addresses only the development of the intake structure design and the components that help the flow to transition into the helix. The design of the helical channel is described in a separate report (Reclamation's report HL-01-2015) [1].

The purpose of this study was to determine inlet geometry and transitions that would provide optimal hydraulic conditions for attracting and guiding juvenile fish into the fish passage system. Both numerical and physical modeling were used to develop and refine the final designs. Throughout the design process, Reclamation collaborated with the Technical Yakima Basin Storage Fish Passage Work Group (Core team) of biologists, engineers, and other specialists from Federal, State, Tribal, and local entities [2]. The Core team evaluated the existing interim flume that uses a stoplog weir and found the fish attraction acceptable but was concerned that the freefall and turbulent flow downstream of the weir was questionable and could cause fish injury. Ultimately, the 6 inlets were generally designed using approach attributes of the existing interim fishway including the upstream training walls. The step by step process in modeling the intake structure with both CFD and physical models provided design team and Core team members with the necessary data to make decisions regarding the final design of the multi-level inlet structure. The final design will include 6 individual inlets, each with an overflow gate (ramp-weir) configured to provide an adjustable weir crest elevation and upstream and downstream ramps. This design provides a gradual velocity gradient approaching the 8 ft/s capture velocity and supercritical open-channel flow conditions from the gate crest into the helix. The dual-ramp gate also ensures continual and gradual increases in flow velocity through the intake structure, with no separated flow regions that might delay passage or disorient fish. As the reservoir water surface rises in elevation each inlet will be operated to provide surface releases (from the upper 10 feet of the reservoir) to attract juvenile fish. The 6 inlets will serve overlapping elevation ranges so that as the reservoir reaches each consecutive level, the inlet gate below will be closed

and only the upper-most inlet, below reservoir water surface, will be operated at any given time.

The multilevel intake structure will be located in Cle Elum Reservoir and will provide downstream fish passage into the helix structure. From the helix, fish and flow will enter a tunnel that extends through the right abutment of the spillway. Finally fish will be released into the river channel near the downstream end of the spillway stilling basin.

# Background

Cle Elum Dam, located on the Cle Elum River about 8 miles northwest of Cle Elum, Washington, was built in 1933 without fish passage facilities (Figure 1 and Figure 2). The dam expanded a natural lake that historically supported populations of three species of salmon (sockeye, coho and spring chinook), steelhead, Pacific lamprey, bull trout and other resident fish. Lack of passage at the dam blocked access to the lake and upstream habitat for anadromous salmonids and contributed to the extirpation of sockeye salmon runs in the Yakima River basin. The absence of passage has also isolated local populations of bull trout and may be preventing their recolonization.[2]

A fish recovery effort has been underway in the Yakima River basin since the 1980s. Reclamation began studying fish passage at the five Yakima Project Dams in 2002 as a result of commitments made to Washington State and the Yakama Nation related to Safety of Dams (SOD) work in the rehabilitation of Keechelus Dam. In 2003 Reclamation completed an appraisal-level assessment of alternatives for providing fish passage at the five major storage dams in the Yakima basin ( Bumping Lake, Tieton, Cle Elum, Kachess, and Keechelus) and identified Cle Elum and Bumping Lake Dams as the highest priority sites for continued investigation of fish passage feasibility.[3]

In 2004 a temporary fish passage structure was constructed to assess whether reintroduced salmonids would effectively find downstream egress through a surface release near the dam. The “interim flume” involved modification of a spillway radial gate and headworks structure, and addition of a wooden flume that ran inside of the main spillway channel. After multiple years of testing, it was determined that juvenile salmonids would locate the passage entrance and volitionally move downstream. However the interim flume was only able to be operated in a 17 foot range between full pool and the spillway crest, which often does not temporally coincide with the optimal juvenile migration period [4].

The relative success of the interim flume and its limitations led the project team to investigate concepts for a more permanent solution with improved performance over a range of reservoir conditions. A Final Planning Report was completed in April 2011, and this launched the design of fish passage systems for Cle Elum Dam. The project’s purpose and need was “to construct fish passage facilities and to maximize ecosystem integrity by restoring connectivity, biodiversity and natural production of anadromous salmonids.” [2]

This collaborative project involves the Bureau of Reclamation (Reclamation), Washington State Department of Ecology (Ecology), Washington State Department of Fish and Wildlife (WDFW), and the Yakama Nation. This project has two components—fish passage facilities design, with Reclamation taking the lead, and a fish reintroduction program developed by the Yakama Nation with assistance from WDFW. Fish species expected to benefit include sockeye, coho and spring chinook salmon, and Pacific Lamprey. The project also benefits the

Upper Middle Columbia River Steelhead and Bull Trout, two species listed as threatened under the Endangered Species Act.

## Introduction

The U.S. Bureau of Reclamation (Reclamation) has completed the development of a downstream passage design for Cle Elum Dam that consists of a series of structures that will allow fish to self-guide into a structure that carries them around the dam and into the downstream river channel. Downstream fish passage at high head dams has always been difficult. Most high dams with downstream fish passage are hydropower generation facilities with minimal fluctuation in pool elevation. Generally, fish passage structures at these facilities consist of manned surface collectors using trap and haul methods that require high operation and maintenance (O&M) costs. Cle Elum Dam is a storage reservoir, and experiences seasonal swings in reservoir water surface elevation of about 100 feet. Surface collectors are not compatible with such large reservoir fluctuations, so new fish passage concepts were developed and evaluated for use at this site.

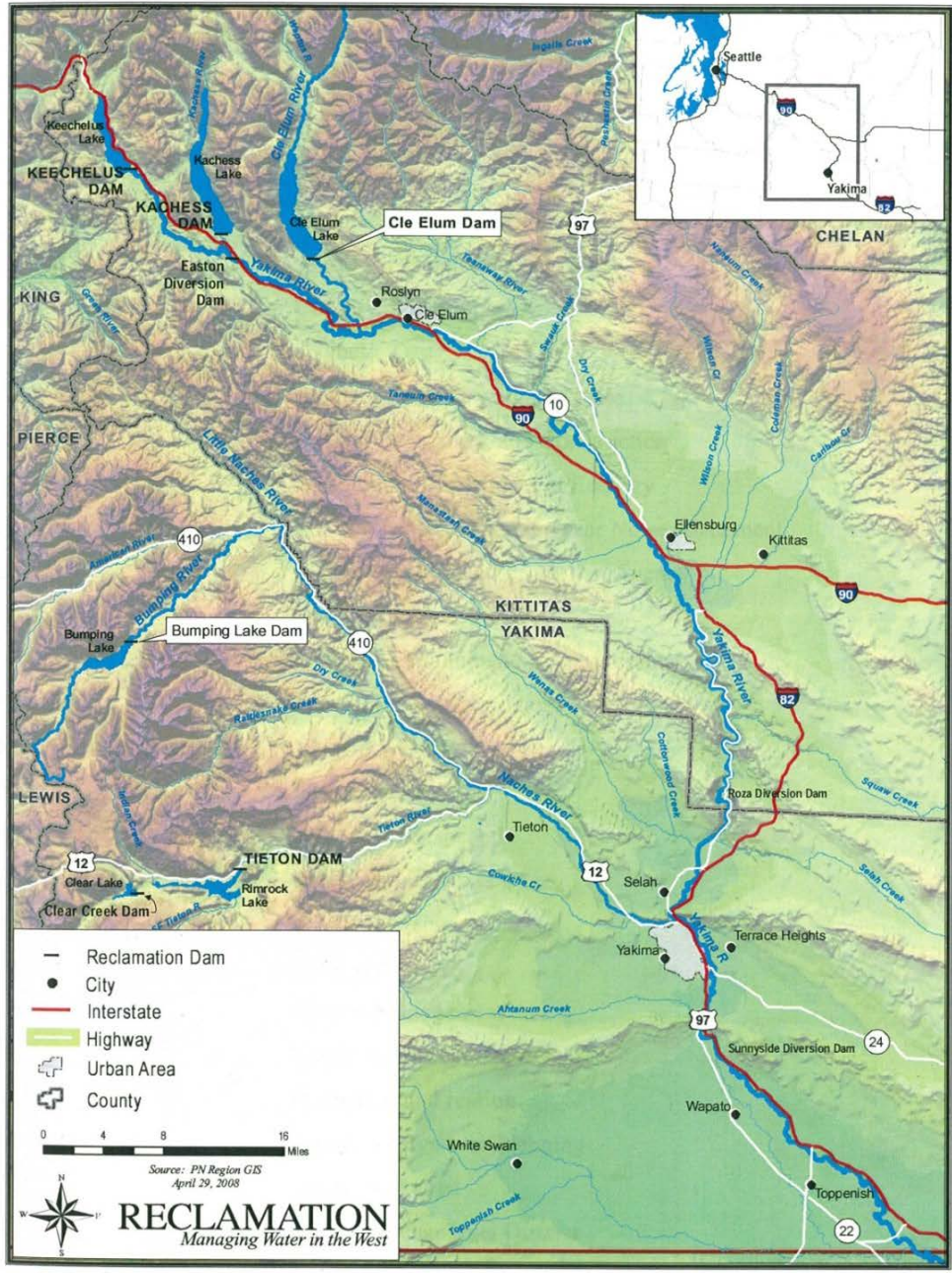
The final design includes an intake structure, helical free-surface fish passage channel (the helix), tunnel, and outfall (Figure 3). Only the development of the intake structure design and the components that help flow transition into the helix are discussed within this report. The helix is described in a separate report (Reclamation Hydraulic Laboratory Report HL-01-2015).

The multilevel intake structure will allow fish passage from Cle Elum Reservoir while the reservoir water surface ranges from a maximum of about 2243.0 ft to a minimum of about 2180.0 ft based on hydrologic studies [2]. The intake structure can draw flow from the reservoir at six different elevations, each vertically separated by 11.75 ft. One of the major challenges in designing the intake structure was that there is varying biological data and opinions with regard to attraction flow fields required to promote downstream movement, and as a result, design criteria are not well established.

Throughout the design process, Reclamation has collaborated with the Technical Yakima Basin Storage Fish Passage Work Group (Core team) of biologists, engineers, and other specialists from Federal, State, Tribal, and local entities to evaluate the effectiveness of the fish passage alternatives and their potential for causing injury to fish.



Figure 1. — Cle Elum Dam and spillway.



Yakima Project Storage Dams, including Cle Elum and Bumping Lake Dams

Figure 2. — Location map of Cle Elum Dam.

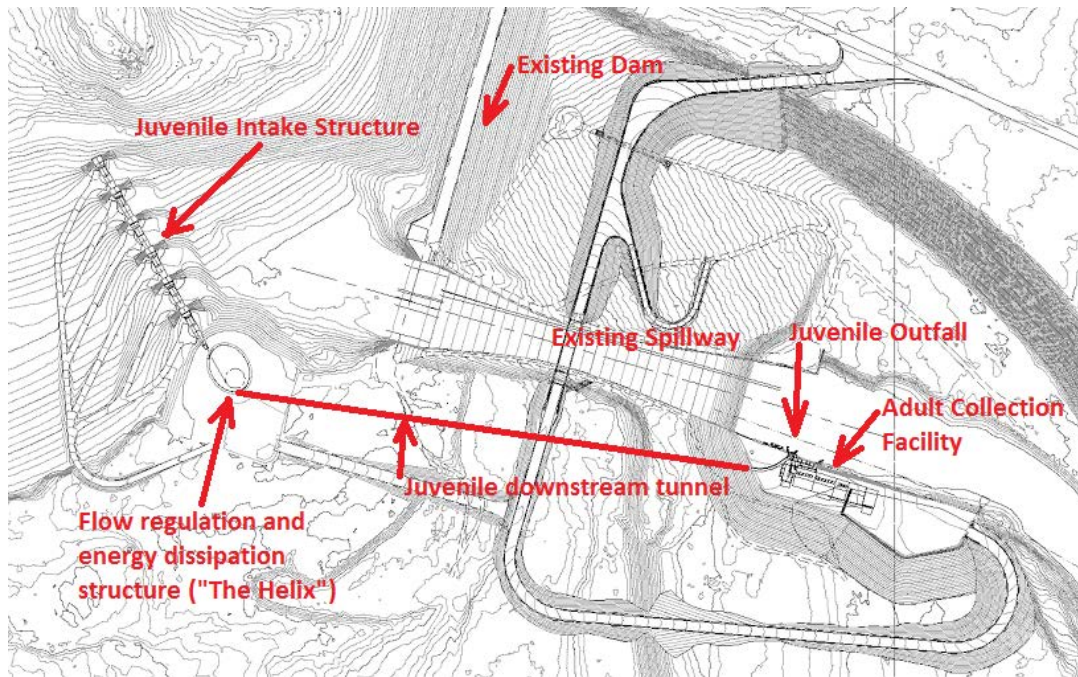


Figure 3. — Layout of proposed intake structure, helix and tunnel through right abutment.

## Model Study Overview

The purpose of this study was to determine intake structure geometry and transitions for providing optimal hydraulic entrance conditions for safe continuous downstream fish passage from the reservoir into the helix during the downstream juvenile salmon passage season. Both CFD (Computational Fluid Dynamics) simulations using FLOW-3D, and physical modeling were used to determine, refine, and optimize options considered for the final design. In addition, the numerical model was used to determine the flow field approaching the inlet for the final design to correlate fish attraction velocities and the size of the zone of influence to discharge. Comparison of physical model and CFD results validated the approach and CFD was used for the final design.

## Operation Criteria

The intake structure will be used to control flow into the helix and will provide enough flow (200 ft<sup>3</sup>/s to 400 ft<sup>3</sup>/s) into the structure to attract juvenile fish (Figure 4). The intake structure was designed to follow the reservoir bank since fish migrating down the reservoir tend to follow the bank's edge. Six separate inlets will be provided so that surface releases from the upper 10 ft of the reservoir can be maintained as the reservoir rises from elev. 2180 ft to 2243 ft (Figure 4).

Design criteria for the intake structure called for a smooth transition of flow into the structure until a capture velocity of 8 ft/s was achieved. Initially the Core team required the intake channel velocity gradient to be less than 1.0 ft/s/ft upstream of the 8 ft/s capture velocity. Several months of testing with the physical model was conducted with inlet designs based on this criterion. The initial designs tested used a bell-mouth type entrance, designed to provide a gradually increasing velocity gradient into the structure. However during the course of the study, more recent research discussed by the Core Team (but not provided to Reclamation) indicated that the 1.0 ft/s/ft gradient criteria was considered too high. Therefore model testing of designs based on this criterion were discontinued. The abandoned studies are described in Appendix B of this document.

Interpretation of the newer research by Core team members suggested that velocity gradients approaching a juvenile downstream passage structure should be in the range of 0.1 ft/s/ft to 0.2 ft/s/ft upstream of the 8 ft/s capture velocity. Implementing this new criterion with a bell-mouth shaped design would have more than doubled the size of the inlet approach structure, making it prohibitively expensive to build. As a result, stakeholders and Core team members made the decision to use a design for an intake structure that would duplicate or improve upon existing approach conditions of the interim flume, since it has shown good success in attracting and passing juvenile fish at Cle Elum Dam since installation in 2005. [4]

The interim fish passage flume was installed on the Cle Elum Dam spillway to demonstrate that flows into the flume would successfully attract juvenile fish before a more permanent structure was constructed. One of the spillway gates was retrofitted in 2005 to provide flow into the flume. The structure consists of three 11-ft wide bays with stoplogs inserted into each bay to act as vertical weirs controlling the amount of flow being pulled from the reservoir into the flume (Figure 5 and Figure 6). Training walls upstream of a vertical weir help straighten the approach flow, and allow shallow flows to approach a normal depth (the ultimate depth in a long channel). As a result, the training wall reduces acceleration at the weir, as opposed to not having a training wall. For this reason, final study models matched the training walls of the interim flume. Flow going over the stoplogs (vertical weir) plunges into a pool and then continues over an Obermeyer gate and into the interim flume (Figure 7). The flume flow carries fish and flow down the spillway where they are discharged into the stilling basin at the base of the spillway (Figure 8). The conveyance channel in this interim system does not meet established fish passage channel velocity criteria, however the Core Team expected the abrasion damage to fish to be minimal where the spillway was smooth. The Core Team considered the hydraulic jump at the exit to be questionable, possibly causing disorientation of fish.

Typically, the interim flume is operated with only the center bay providing passage. Observations during downstream migration periods indicated that a head of about 4 feet above the weir crest optimized fish passage over the crest. Therefore as the reservoir typically rises in the spring which is during the

downstream fish runs, stoplogs are added to maintain a head on the weir that is close to that level. Attraction of fish into the interim flume proved to be successful, however the flume can only be operated when the reservoir elevation is above the crest of the spillway (2240 ft). Thus, the decision was made to develop a more permanent fish passage system with multiple intakes that could be operated at a wide range of reservoir elevations and with a fish conveyance channel that would nearly match the velocity conditions of the interim flume and would be free of hydraulic jumps.

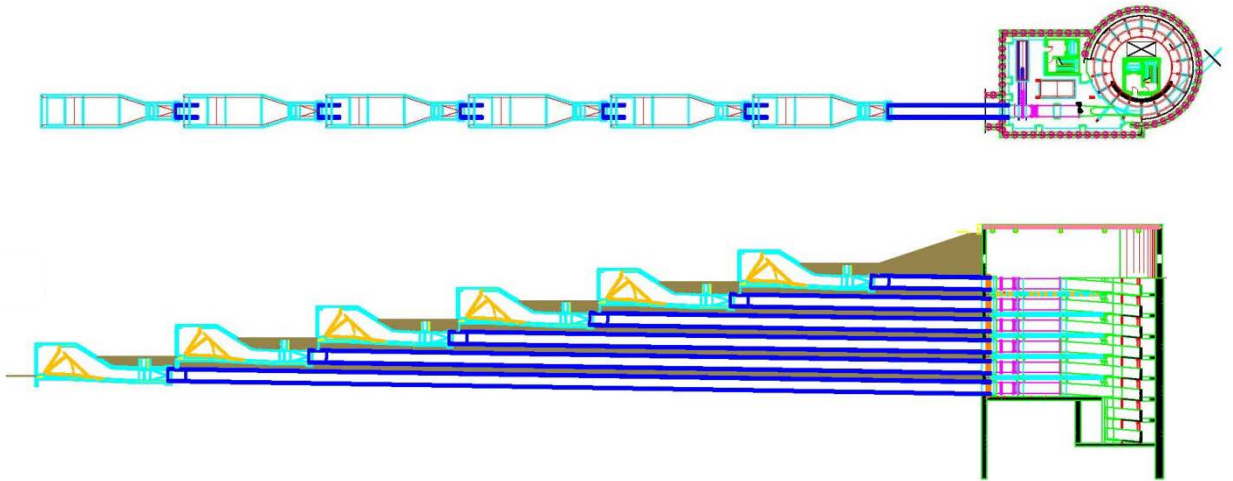


Figure 4. — Intake structure concept with six separate inlets controlling flow into the helix.

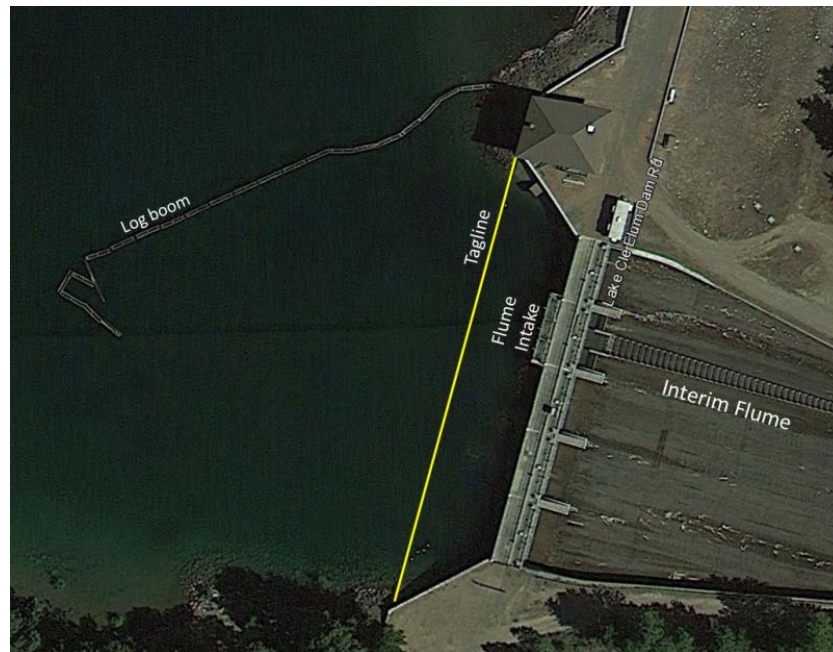


Figure 5. — Looking down on the interim flume near the top of the spillway at Cle Elum Dam.



Figure 6. — Stoplog bays used to control flow into the interim flume. Operators have observed the best fish attraction when the flow is only through the center bay.



Figure 7. — View from the deck above the stoplog structures looking at the upstream side of the Obermeyer gate at interim flume entrance. The gate is downstream from the stoplog bay (located under the deck at the bottom of the image).



Figure 8. — Flow discharging from the interim flume into the stilling basin.

## CFD modeling methods

In order to get an expanded look at the attraction flow field in the reservoir, a computational fluid dynamics (CFD) model using FLOW-3D was used. FLOW-3D is a commercially available computational modeling system. A description of FLOW-3D and the parameters used in Cle Elum modeling are in Appendix A.

## Physical modeling methods

The purpose of the physical model was to:

- Verify the performance of the numerical model, as applied to the simulations of the interim flume entrance, and refine it if necessary, since several assumptions were made when constructing the numerical model. This step was important to ensure that the CFD model could provide an accurate representation of the helix structure intake design.
- Evaluate flow conditions entering the helix structure inlet channels to ensure no excessive turbulence or sloshing.

A 1:9.5 geometric scale was used to construct the model. Similitude between the model and the prototype is achieved when the ratios of the major forces controlling the physical processes are the same in the model and prototype. Since gravitational and inertial forces dominate open channel flow, Froude scale similitude was used to establish a kinematic relationship between the model and

the prototype. The Froude number, which represents the ratio of inertial to gravitational forces, is

$$F_r = \frac{v}{\sqrt{gd}}$$

where  $v$  = velocity,  $g$  = gravitational acceleration, and  $d$  = flow depth. When equal Froude numbers are maintained between the model and the prototype, specific scaling relationships exist between model and prototype values of key flow parameters. In the equations that follow, the  $r$  subscript refers to the ratio of the prototype and model values:

Length ratio:  $L_r = L_m/L_p = 9.5$

Velocity ratio:  $V_r = L_r^{1/2} = (10)^{1/2} = 3.08$

Discharge ratio:  $Q_r = L_r^{5/2} = (10)^{5/2} = 278.17$

## Preliminary Inlet Structure Studies

Several physical models of intake design concepts were tested at the beginning of the study. All of these tests used the velocity gradient guideline of 1.0 ft/s/ft upstream of the 8 ft/s capture velocity and found undesirable conditions in the flow field. These results are documented in Appendix B.

Subsequently the Core team considered new research that suggested that 0.1 ft/s/ft to 0.2 ft/s/ft would be more acceptable. The Core Team also evaluated the existing interim flume that uses a stoplog (vertical) weir and found the fish attraction acceptable. The guidelines that had velocity gradients that were 1.0 ft/s/ft or 0.1 ft/s/ft to 0.2 ft/s/ft were less acceptable to the Core team since the interim flume was proven acceptable for the fish of concern at Cle Elum.

The Core team was concerned that the freefall and turbulent flow downstream of the interim vertical weir was questionable and could cause fish injury. Accordingly, the 6 inlets were generally designed using approach geometry of the existing interim flume including the upstream training walls. For operational and maintenance purposes, the vertical weir was replaced with a ramp-weir with a downstream ramp to improve the downstream conditions.

This study used CFD and physical modeling to verify the approach conditions, of the interim flume, and used proposed topography in CFD simulations of the proposed intakes.

## Interim flume CFD modeling

After the Core Team agreed that the approach conditions to the interim flume were acceptable, one of the first steps in the redirected design process was to study that flow field. In order to get an extensive look at the flow field for various reservoir water surface elevations, a computational fluid dynamics (CFD) model using FLOW-3D was used (Appendix A). The CFD model was set up to replicate the geometry of the stoplog bay with the center bay operating (Figure 9). Four simulations were run with a 4 foot flow depth over the center weir with weir heights of 0.0 ft, 2.0 ft, 4.0 ft, and 6.0 ft, and resulted with flow rates of 264 ft<sup>3</sup>/s, 308 ft<sup>3</sup>/s, 320 ft<sup>3</sup>/s and 324 ft<sup>3</sup>/s respectively. Centerline profiles for each simulation are shown in Figures 10-13. Velocity fields and velocity gradients were extracted from 2 ft below the reservoir water surface at the center-bay centerline and are plotted in Figures 14-17. The x axis represents station number, with the upstream face of the weir positioned at station 2+96 (ft). The blue line represents velocity (left vertical axis) as a function of station number and the red line (right axis) represents the velocity gradient as a function of station number. On each figure the vertical purple line represents the location where the bay training wall begins, at station number 4+91. The vertical green line intersects the velocity line at capture velocity (8 ft/s) so that the velocity gradient at capture velocity can be identified. The vertical weir or stoplog slot is displayed in dark blue. In each case, although velocity gradually increases to capture velocity, the velocity gradient decreases but is still positive within the training walls. This decrease demonstrated the importance of having training walls in the effort to duplicate interim flume conditions. Maximum velocity gradient before reaching capture velocity ranges from 1.15 ft/s/ft to 1.45 ft/s/ft. Observations at Cle Elum dam indicate that juvenile fish passage is successful under each of the flow conditions identified in Figures 14 through 17.

Study of the results generally indicates the lower the flow depth to training wall length ratio, the more the velocity gradient will be reduced by having training walls. But since the velocity gradient stays positive for these conditions, the velocity still increases as the flow travels towards the weir causing positive attraction characteristics for fish. For high flow depth to training wall length ratios the rate of velocity gradient increase is maintained. So the designers chose to use the interim training wall configuration as much as possible considering the weir for the proposed design includes an adjustable ramp.

Next, a physical model was used to verify the results from the CFD model.

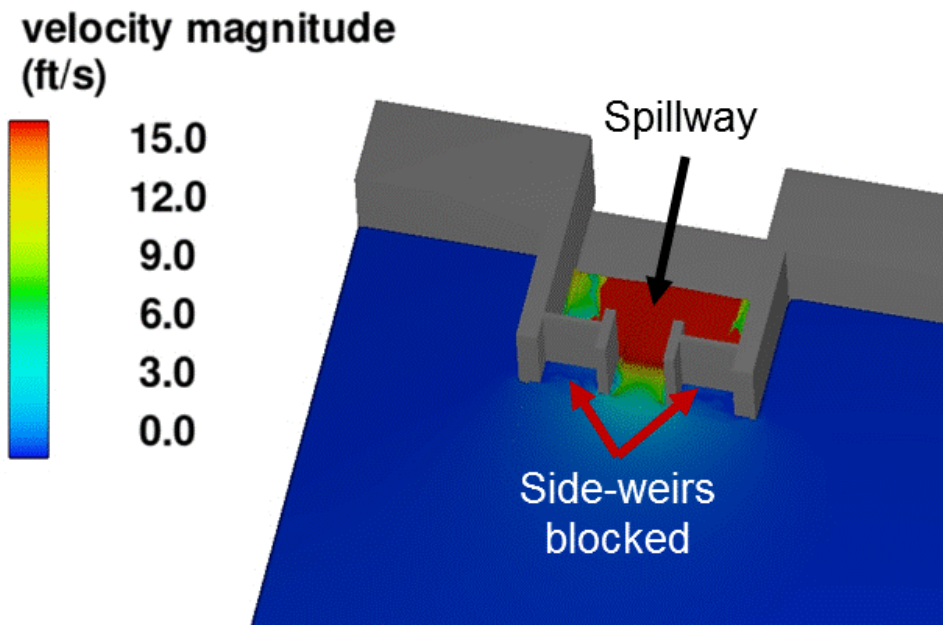


Figure 9. — CFD model representing flow through center stoplog bay for the interim flume.

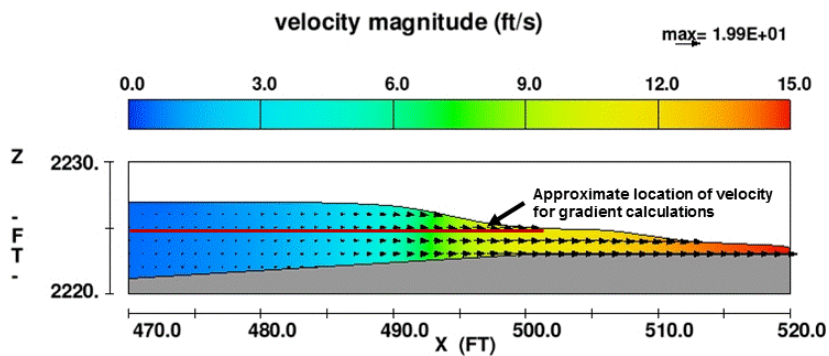


Figure 10. — Flow profile at centerline of center stoplog bay at 264 ft<sup>3</sup>/s with no stoplogs installed. The Obermeyer gate downstream of the stoplog slot is in the down position, and does not affect flow conditions.

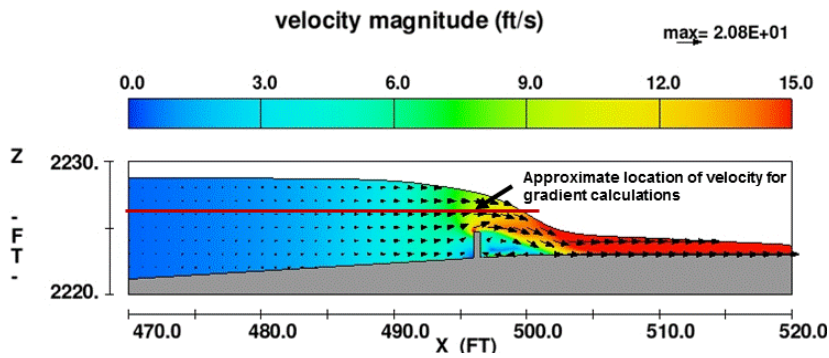


Figure 11. — Flow profile at centerline of center stoplog bay at 308 ft<sup>3</sup>/s with stoplogs installed to a height of 2 ft. Reservoir water surface elevation is 4 ft above the weir crest. The Obermeyer gate downstream of the stoplog does not affect approach conditions and was not modeled.

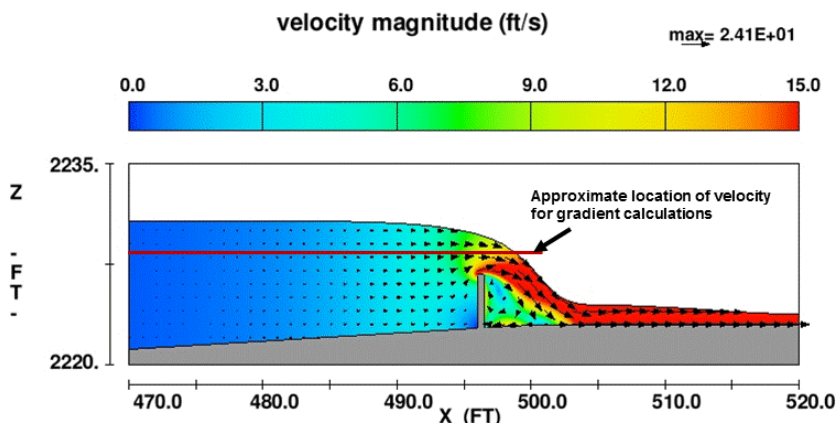


Figure 12. — Flow profile at centerline of center stoplog bay at 320 ft<sup>3</sup>/s with stoplogs installed to a height of 4 ft. Reservoir water surface elevation is 4 ft above the weir crest. The Obermeyer gate downstream of the stoplog does not affect approach conditions and was not modeled.

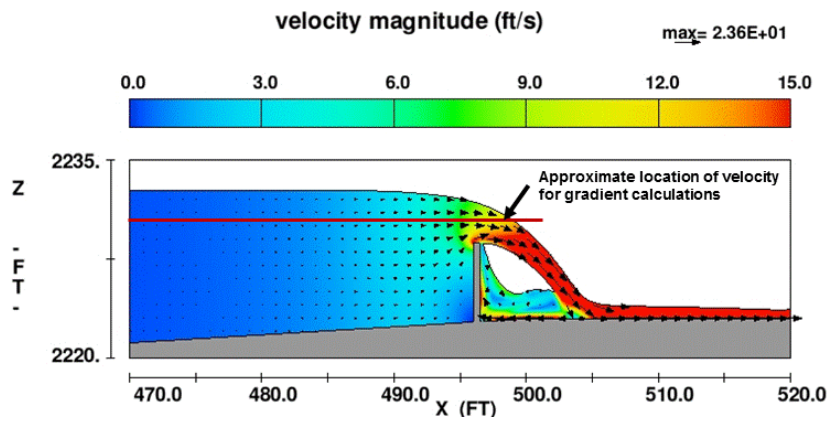


Figure 13. — Flow profile at centerline of center stoplog bay at 324 ft<sup>3</sup>/s with stoplogs installed to a height of 6 ft. Reservoir water surface elevation is 4 ft above the weir crest. The Obermeyer gate downstream of the stoplog does not affect approach conditions and was not modeled.

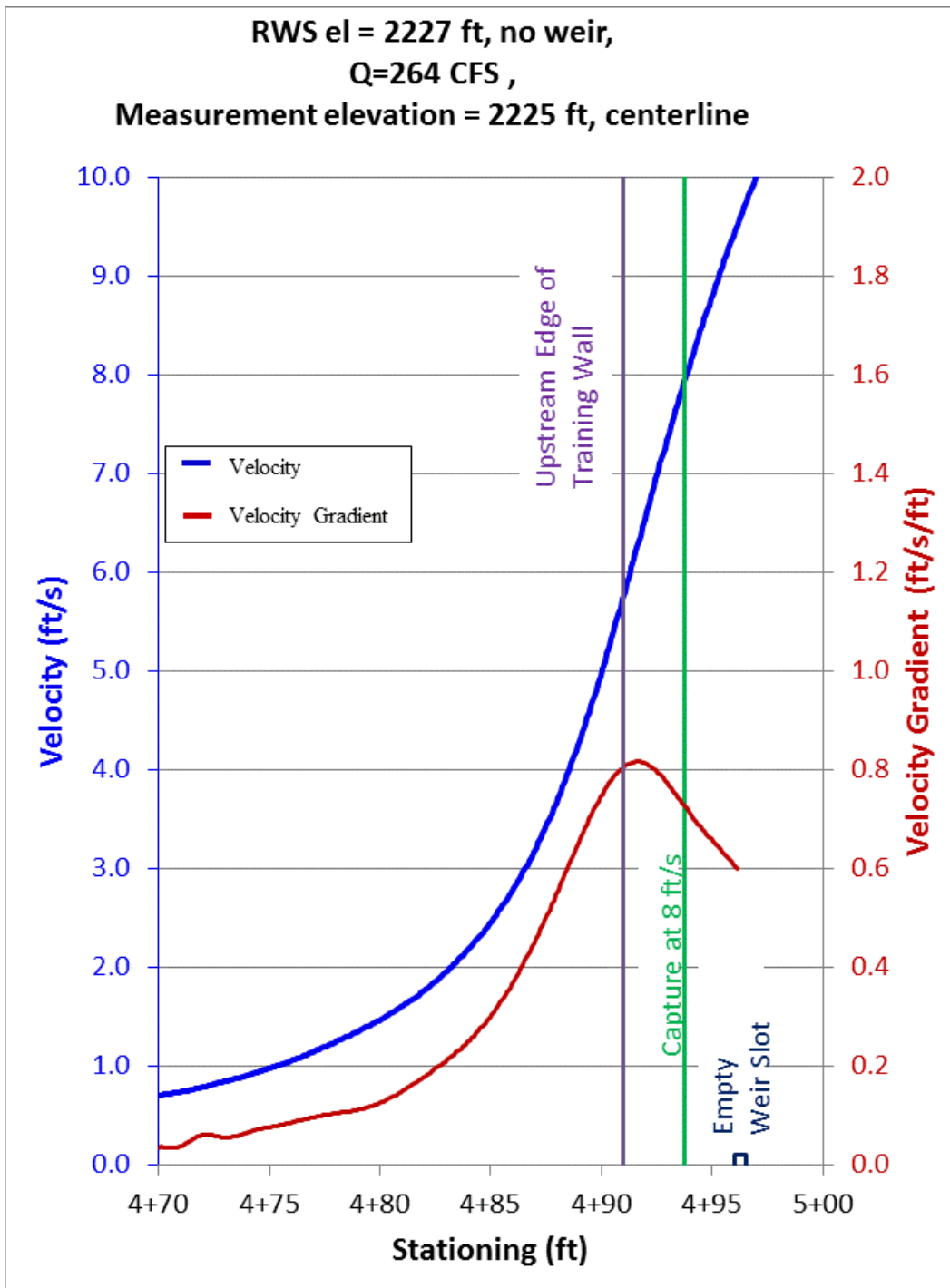


Figure 14. — Velocity and velocity gradient determined from the CFD model at 2 ft below water surface along the centerline of the center stoplog bay with no stoplogs installed. Discharge into flume is 264 ft<sup>3</sup>/s.

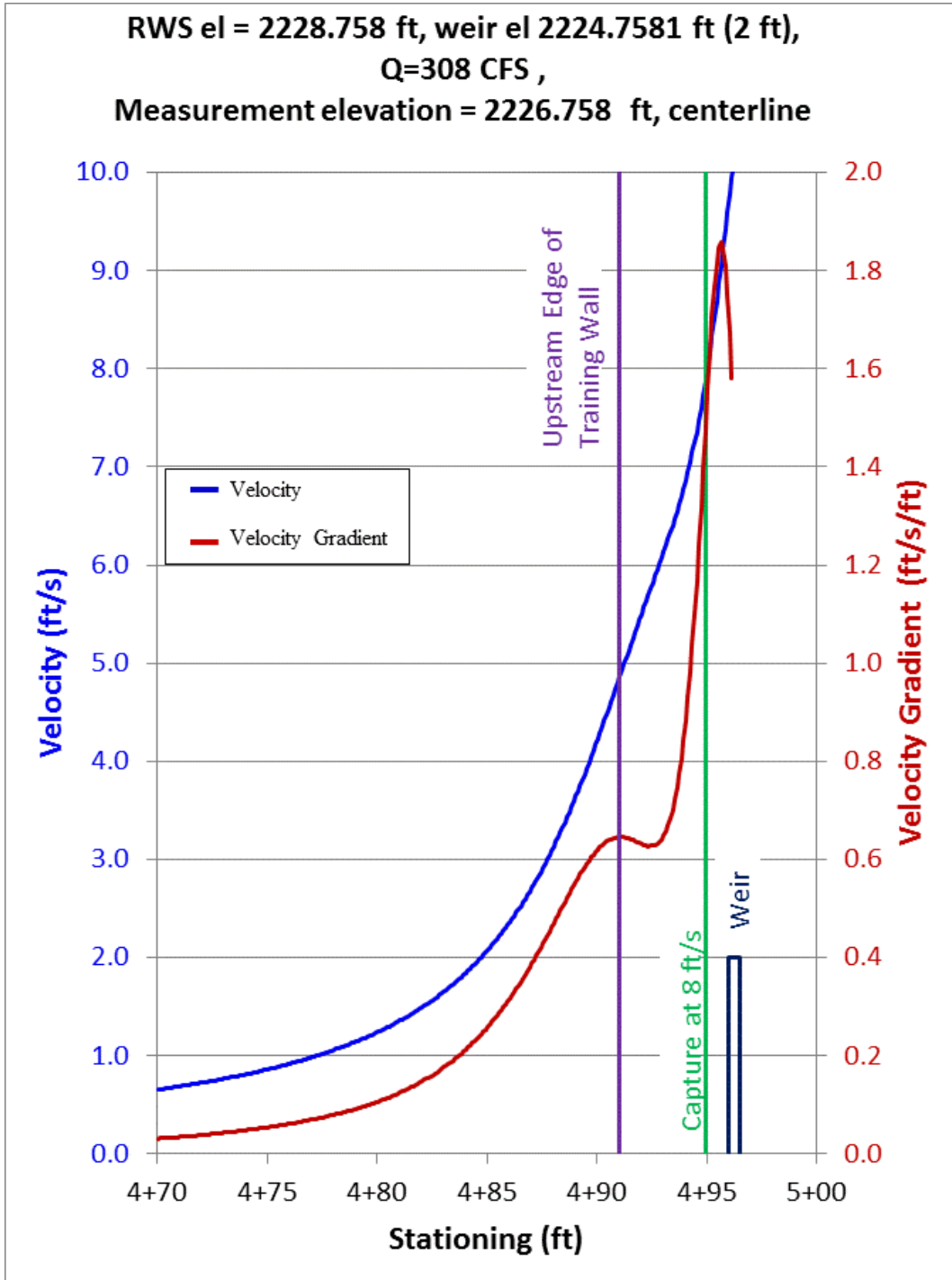


Figure 15. — CFD velocity and velocity gradient 2 ft below water surface along the centerline of the center stoplog bay with stoplogs installed to a 2 ft height. Discharge into flume is 308 ft<sup>3</sup>/s.

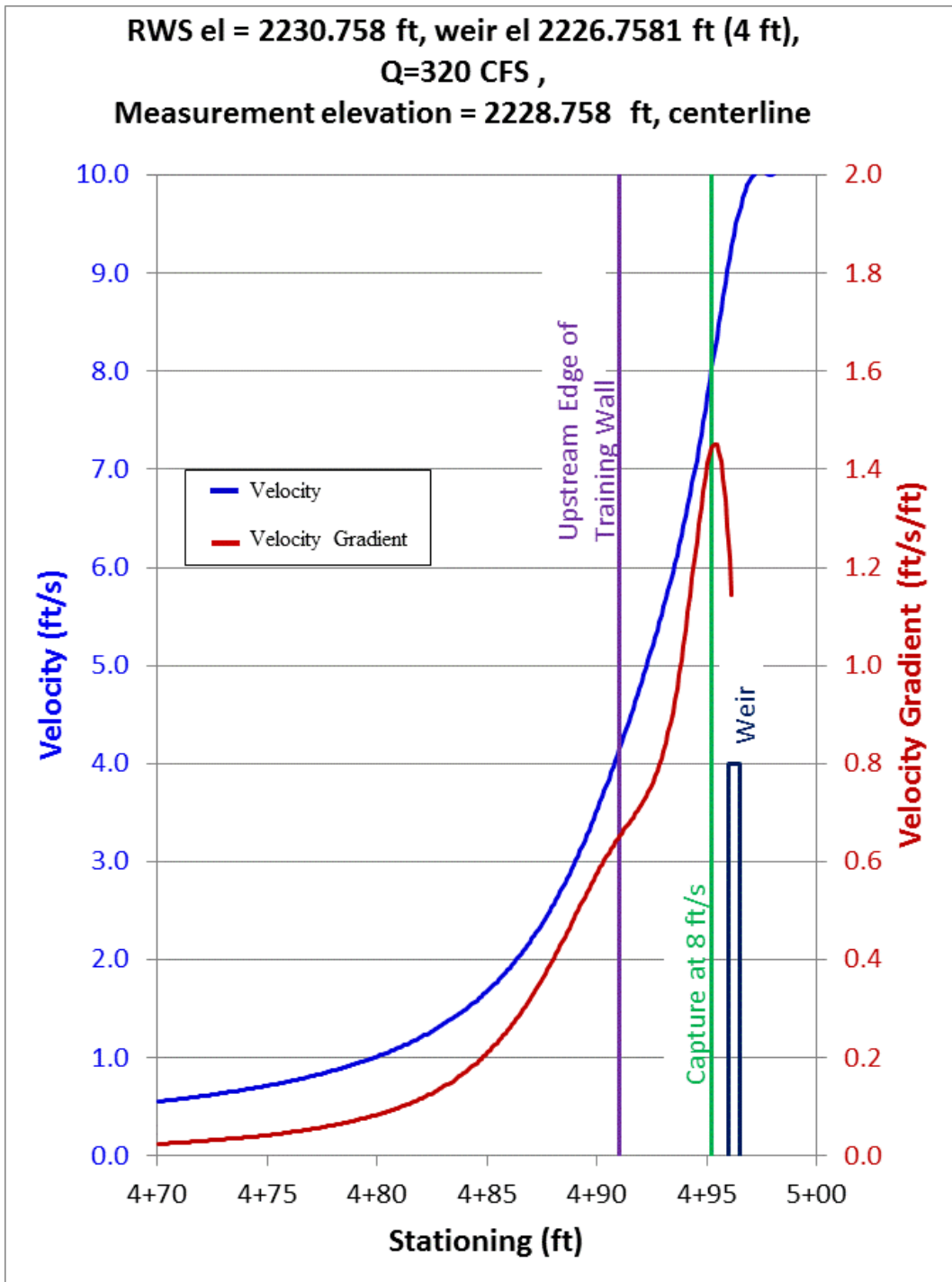


Figure 16. — CFD velocity and velocity gradient 2 ft below water surface along the centerline of the center stoplog bay with stoplogs installed to a 4 ft height. Discharge into flume is 320 ft<sup>3</sup>/s.

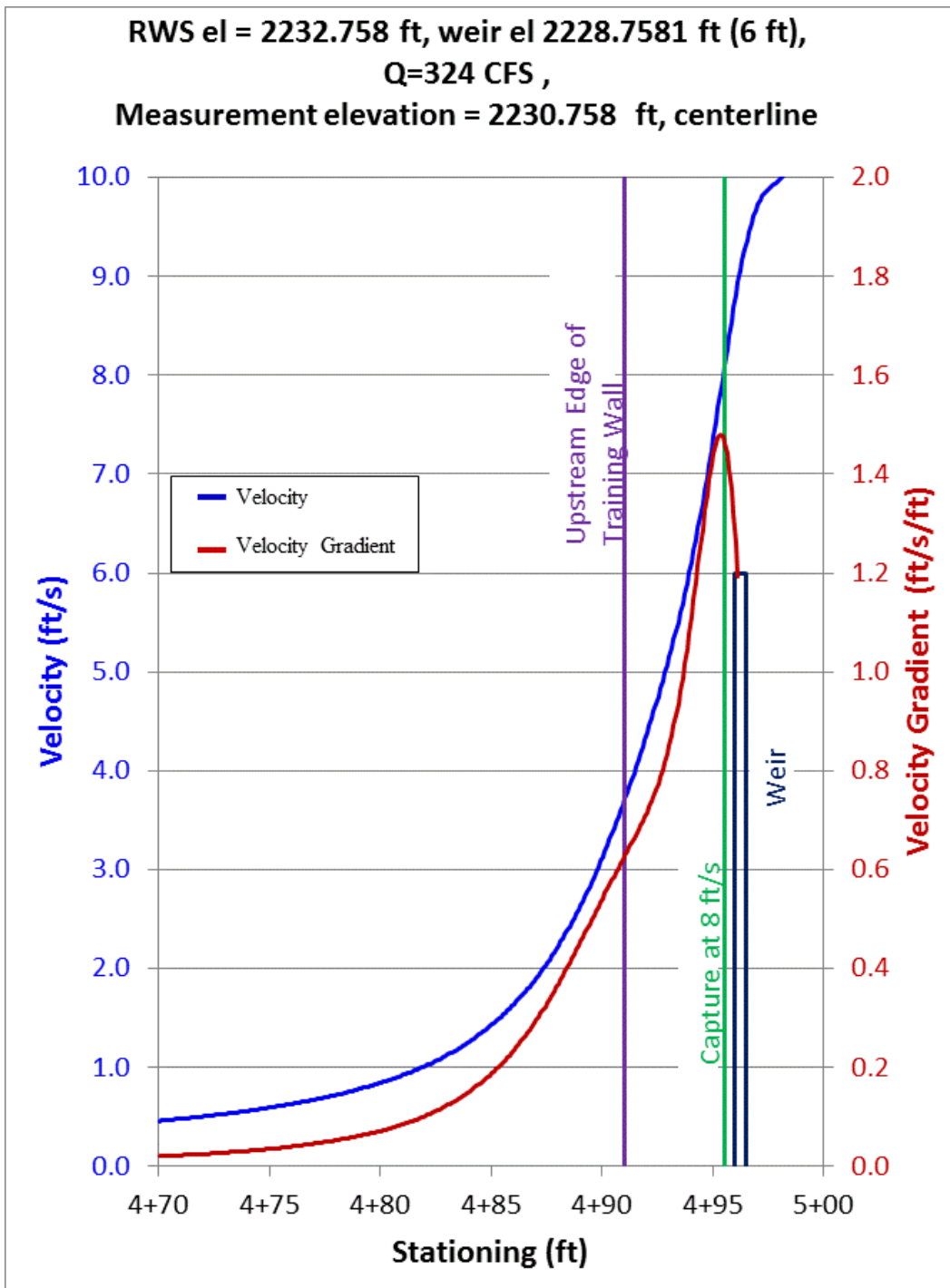


Figure 17. — CFD velocity and velocity gradient 2 ft below water surface along the centerline of the center stoplog bay with stoplogs installed to a 6 ft height. Discharge into flume is 324 ft<sup>3</sup>/s.

## **Interim flume physical modeling**

The 11 ft wide center-bay entrance structure for the interim flume was constructed in the physical model to determine existing approach conditions (Figure 18). Velocities approaching the weir were measured with a Sontek ADV probe. Figures 19 and 20 compare velocity and velocity gradients measured 2 ft below the water surface, at the bay centerline, at a flow of 320 ft<sup>3</sup>/s for the CFD and physical model. Results are similar between the CFD and physical model, however the gradient drops off to a greater degree in the physical model once flow reaches the training walls.

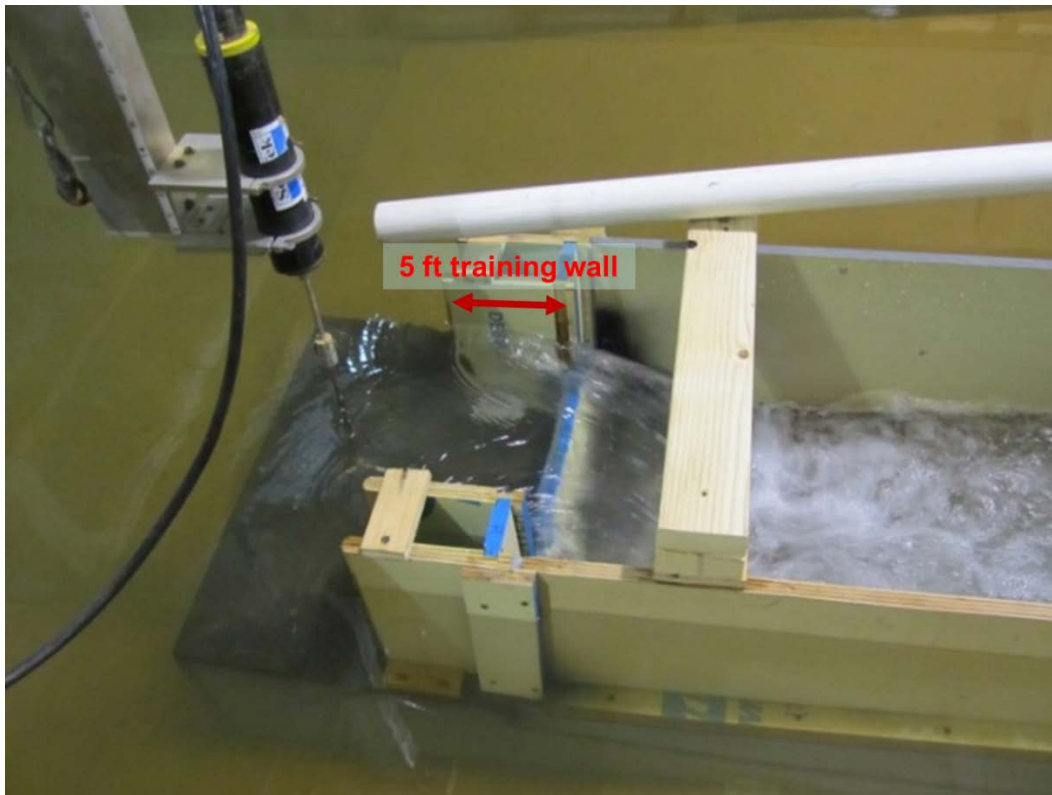


Figure 18. — Physical model of the interim flume with a 4-ft high vertical weir spanning a width of 11 ft.

RWS el = 2230.7581 ft, weir el 2226.7581 ft (4 ft),  
 Q=320 CFS,  
 Measurement elevation = 2228.7581 ft, centerline

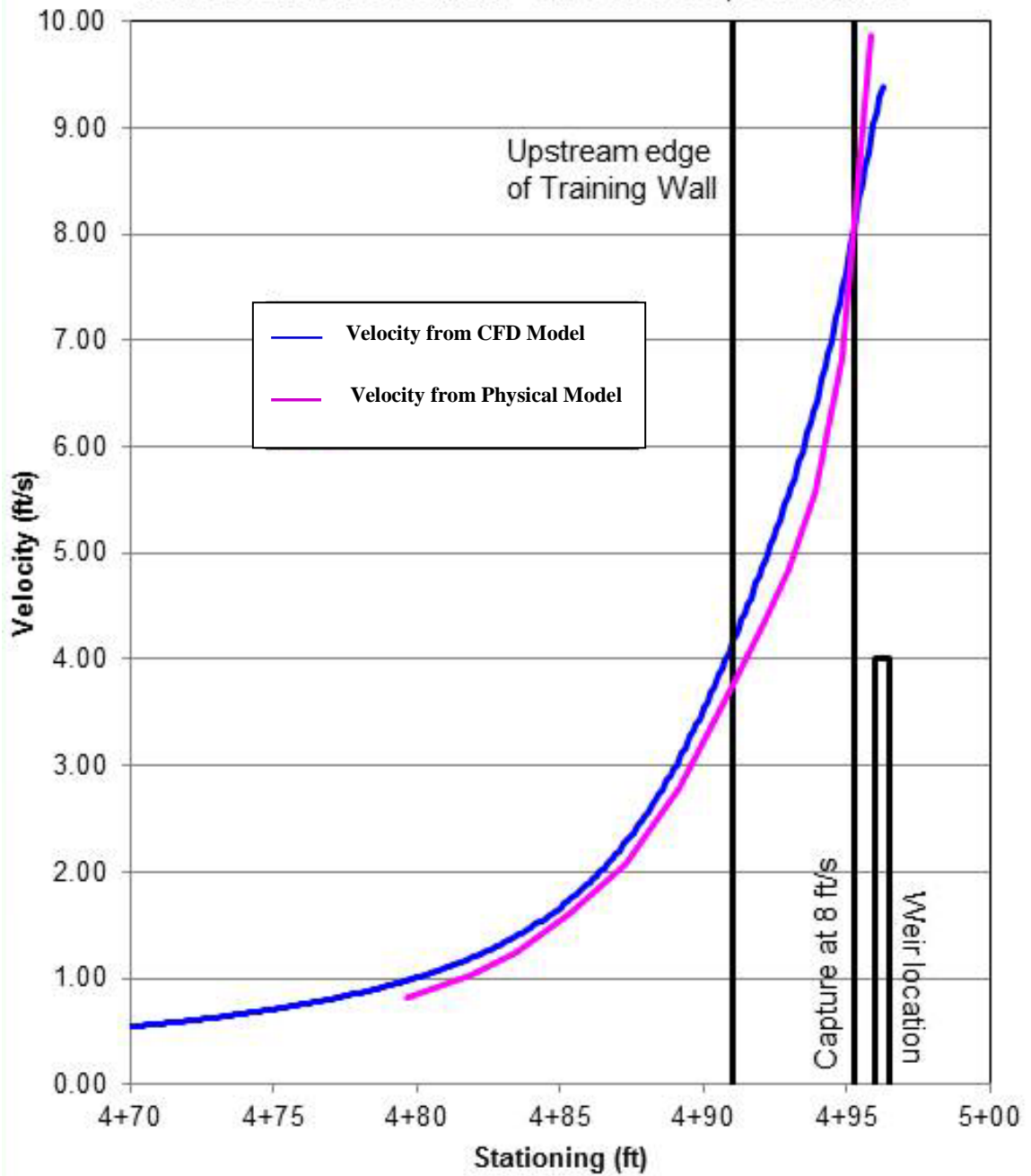


Figure 19. — Comparison of physical (pink) and numerical modeling (blue) data for velocities measured 2 ft below the water surface at the bay centerline for 320 ft<sup>3</sup>/s.

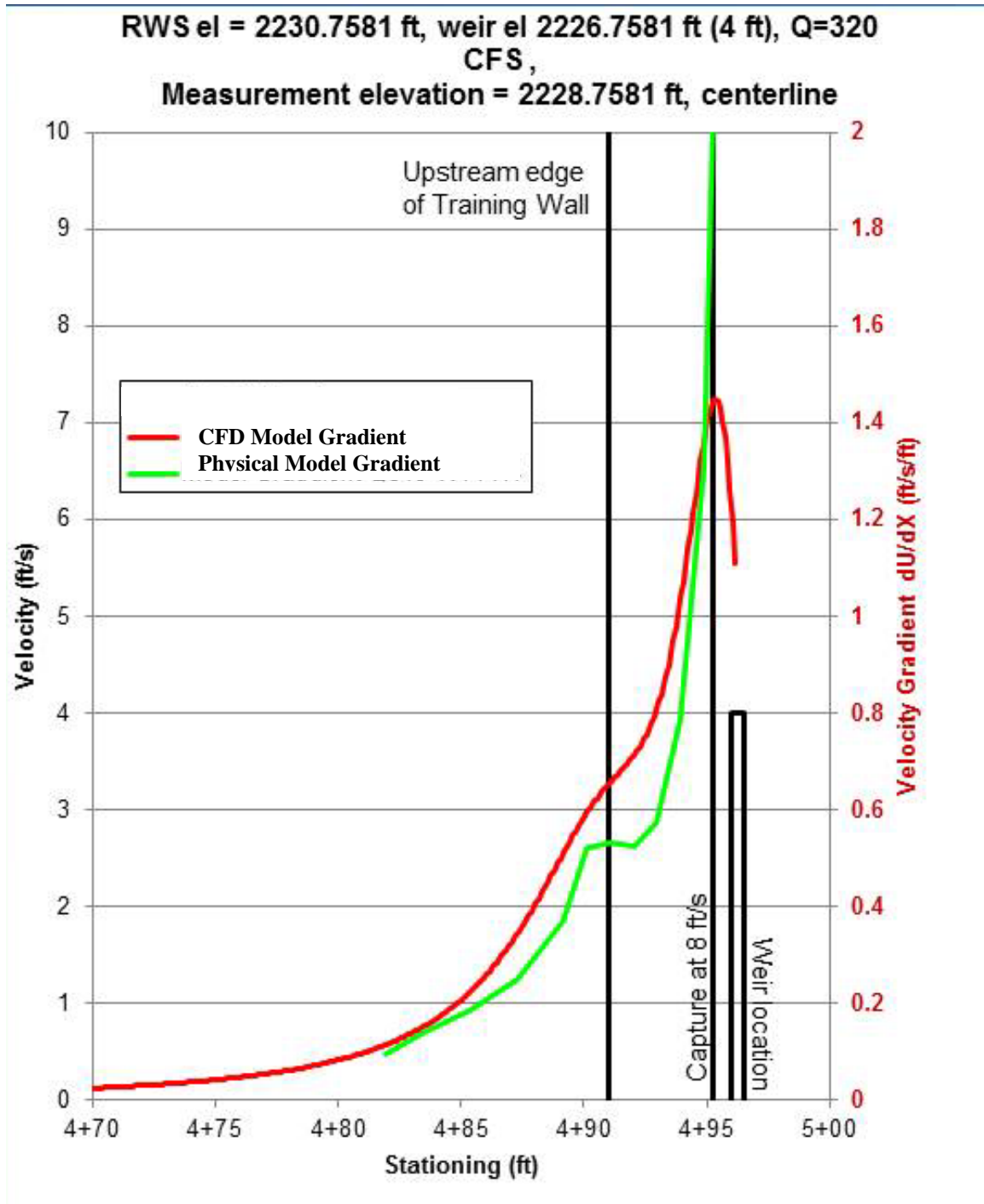


Figure 20. — Comparison of physical and numerical modeling data for velocity gradients measured 2 ft below the water surface at the bay centerline for 320 ft<sup>3</sup>/s.

## Weir and ramp-weir tests

Once the flow conditions entering the interim flume were well understood, testing was performed to develop an intake design that could be applied to each of the multi-level intakes needed for the helix structure. Tests were conducted with several weir heights in both a vertical weir configuration similar to the stoplog weir entrance to the interim flume and with an upstream ramp attached to each weir (ramp-weir configuration) to determine the effect of a ramp on the intake velocity field and velocity gradients. The tests were conducted with a weir that spanned the 17 ft width of the originally proposed design inlet structure trough, since this configuration was readily available (Appendix B). Side walls were added to the inlet trough section to prevent side-weir overflow, but training walls upstream from the weir crest (like those in the final inlet configuration) were not included in this series of tests. Because this inlet configuration varied significantly from the final inlet configuration discussed in the next section, the details of these tests are reported only in Appendix C.

Two significant conclusions were drawn from this series of tests:

- Addition of a ramp upstream from the weir crest led to a more gradual increase in velocity gradient approaching the crest and allowed the capture velocity of 8 ft/s to be reached at or upstream from the weir crest. With vertical weir configurations the capture velocity was not reached until after the flow passed over the weir crest. The Core team found the vertical weir configuration undesirable because it could allow fish to escape back to the reservoir even when they had reached the crest of the weir.
- The addition of a downstream ramp was also found to be desirable. Without a downstream ramp, the flow over the weir becomes an impinging jet that creates the potential for fish to strongly impact the floor of the channel. Testing was conducted to evaluate the effect of using a fish-friendly control valve (pinch valve) to throttle flow and create a cushioning tailwater pool and submerged hydraulic jump below the vertical weir, but turbulence associated with the hydraulic jump made this an undesirable solution. A downstream ramp allows a smoother transition of flow from the weir crest to the helix. Tests described in the next section (Final Inlet Configuration) were used to ensure that supercritical flow would be maintained all the way into the helix structure (no hydraulic jump).

## Final Inlet Configuration

The step by step process of modeling the intake structure design, with varying and sometimes conflicting criteria, using both CFD and physical models, provided the design team and Core team members with the necessary data to make decisions

regarding the final design of the multi-level intake structure. The final design for the structure (Figure 21) includes 6 individual inlets (Figure 22) each with an adjustable height ramp-weir at the entrance to regulate the flow rate into the helix as the reservoir level varies through each inlet's operating range (Figure 23). Each weir is configured as an inclined overflow gate (Obermeyer), with the gate forming an upstream ramp that allows flow to gradually accelerate as it approaches the gate crest (Figure 24). This maintains velocity gradients in a range comparable to those that exist in the interim flume entrance which was found to be acceptable to both the Design and Core Teams. The final design also includes a downstream ramp attached to the crest of the gate to maintain supercritical open-channel flow conditions from the gate into the helix for all flow depths downstream of the gate crest. As the reservoir rises in elevation each inlet will be operated to provide surface releases from the upper 10 feet of the reservoir to attract juvenile fish. The operating ranges of the 6 inlets will be overlapped in elevation so that as the reservoir reaches each consecutive level, the inlet gate below can be closed and only the upper-most inlet, below reservoir level, will be operated at any given time.

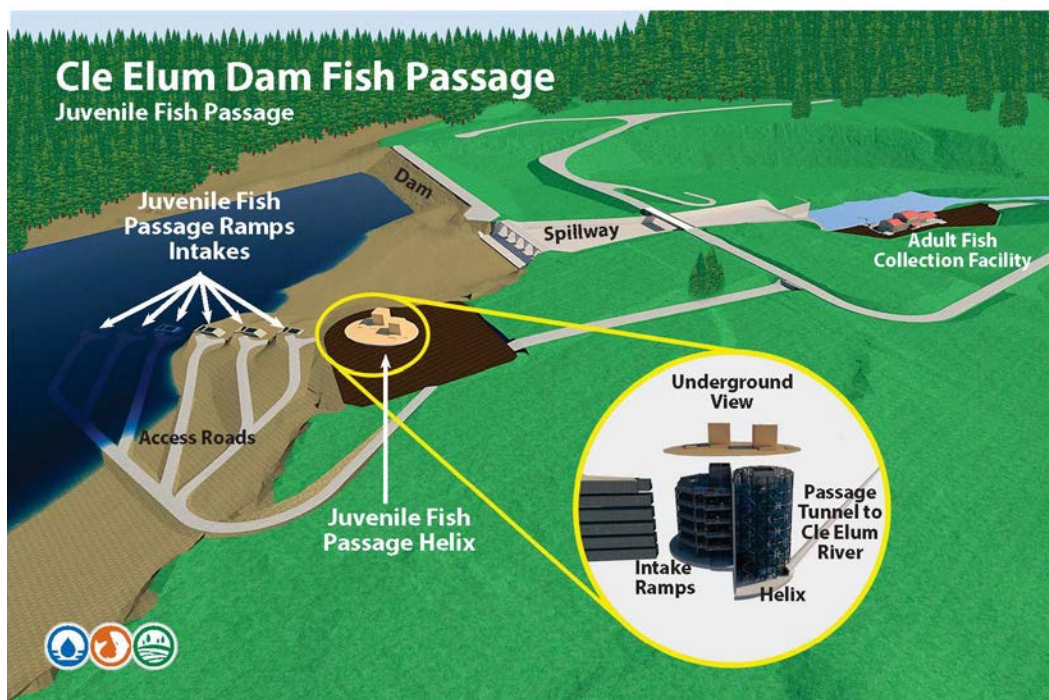


Figure 21. — Final design juvenile fish passage structure overview.



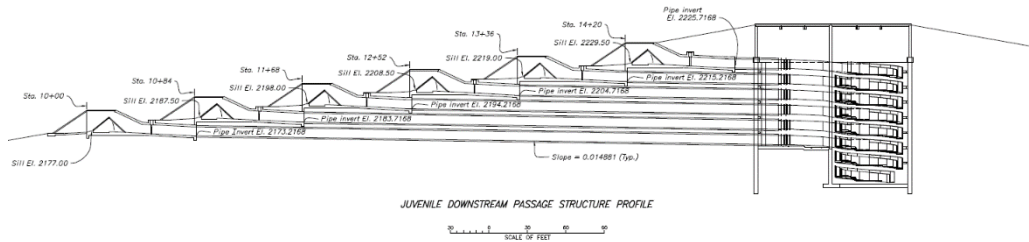


Figure 24. — Profile view of the juvenile fish passage inlets and helix structures.

Incorporating the adjustable upstream ramp into the weir-gate design and adding upstream training walls to the structure produced significant improvements in the approach flow conditions. Figure 25 compares velocity gradients (2 ft below the water surface at the bay centerline) with and without an upstream ramp for a weir length and height of 17 ft and 2.375 ft respectively. The data points in green represent the velocity gradient without an upstream ramp (vertical weir) while the pink data points show the velocity gradient measured at the same location after an upstream ramp was attached. The figure shows that with the ramp attached the gradient increases more gradually. Without the ramp, the gradient stays very low until flow is near the crest of the weir and then it increases significantly. Therefore, by attaching both an upstream ramp and adding training walls to the structure, the velocity gradient will increase more gradually than for a vertical weir alone.

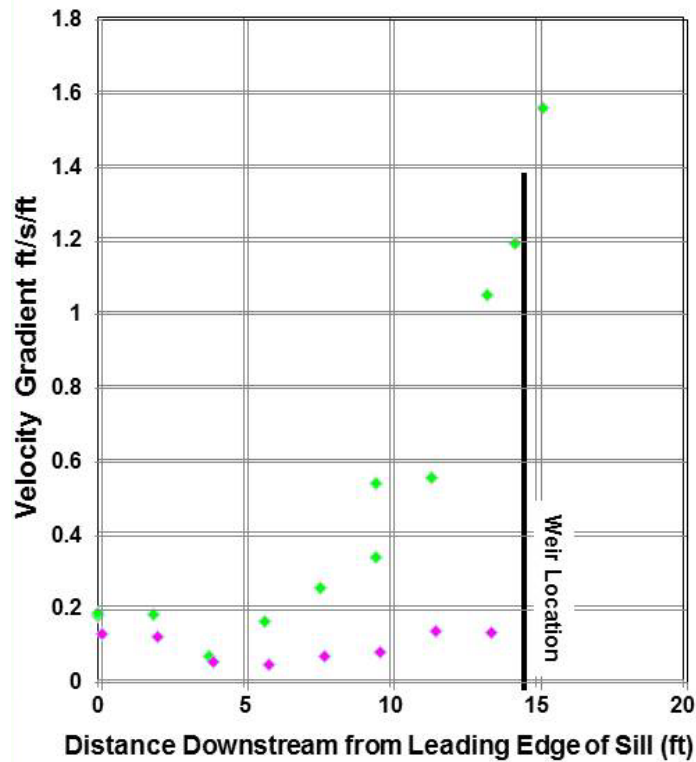


Figure 25. — Comparison of velocity gradients in the physical model with (pink) and without (green) an upstream ramp attached to the weir, using a weir height of 2.375 ft at 200 ft<sup>3</sup>/s.

The final step in the investigations was to use the CFD model to evaluate the velocity field approaching the final intake structure design. This modeling effort included the final reservoir bank topography around the intakes and geometric details of the overlapping inlets and their associated trashrack structures. Two gate positions were simulated to represent two extreme flow cases, both with the reservoir water surface 4 feet above the highest elevation of the gate, which was estimated to discharge 400 ft<sup>3</sup>/s. Setting the actual inflow discharge into each simulation would have caused very long run times as surges within the reservoir settled out. This method also has the increased complication that the inflows and velocity distribution at the three reservoir inlet boundaries are unknown. To overcome these issues, the reservoir level and initial flow conditions were set, and the CFD simulation was then used to discover the resulting discharge. While 4 foot overtopping depth was estimated to achieve 400 ft<sup>3</sup>/s discharge, the resulting discharges were around 18 percent higher (Table 1).

Table 1. Simulated flow conditions for the proposed inlet.

Parameter	Gate-down	Gate-up
Controlling gate elevation	2199.21 ft	2211.1 ft
Reservoir Water surface	2203.21 ft	2215.10 ft
Discharge	474 ft <sup>3</sup> /s	468 ft <sup>3</sup> /s

Critical features investigated in the final design were attraction water velocities within the reservoir, velocity gradients within the intake structure, flow conditions downstream of the ramp-weir, and the transition into the helix structure (Figure 26).

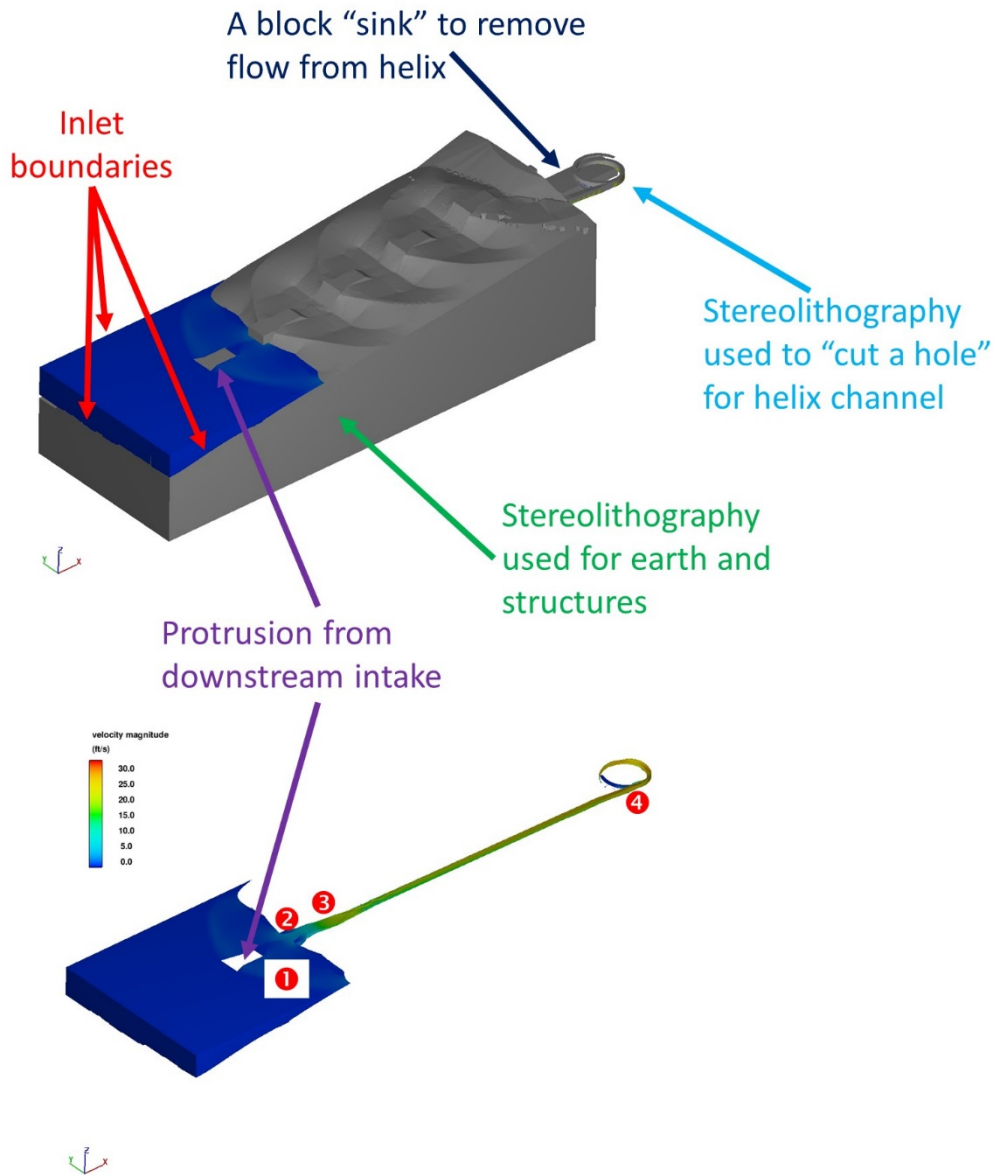


Figure 26. — Overview of simulation with stereolithography (top) and without stereolithography (bottom). Critical features investigated from this design are labeled on the bottom image: ❶ attraction water velocities within the reservoir, ❷ velocity gradients within the intake structure, ❸ flow conditions downstream of the ramp-weir, and ❹ the transition into the helix structure.

## Attraction water velocities within the reservoir

The Design and Core Teams identified that juvenile sockeye salmon have a tendency to swim close to the reservoir bank and within the top 10 feet of the

reservoir in search of a passage downstream. Juvenile sockeye salmon sense a downstream passage from increased water velocities, velocity gradients, and turbulence approaching the downstream passage. Juvenile sockeye salmon may avoid abrupt changes to these conditions.

Any single intake will be used over a range of reservoir levels, and the flow conditions approaching each intake will be affected by the next lower intake structure in the reservoir. To explore performance across a range of conditions, simulations were conducted at the minimum and maximum reservoir levels associated with the use of the middle intake #3. The minimum depth simulation corresponds to the gate-down scenario. Simulations showed that the shallow approach flow depths combine with a minor ridge to the sides of the next downstream intake to produce a peak velocity around 1.0 ft/s (Figure 27). This is expected to provide a wide but gentle attraction field guiding fish towards the intake. Since the simulated discharge was 474 ft<sup>3</sup>/s, peak velocities should be around 0.8 ft/s in this region when the intake operates at 400 ft<sup>3</sup>/s.

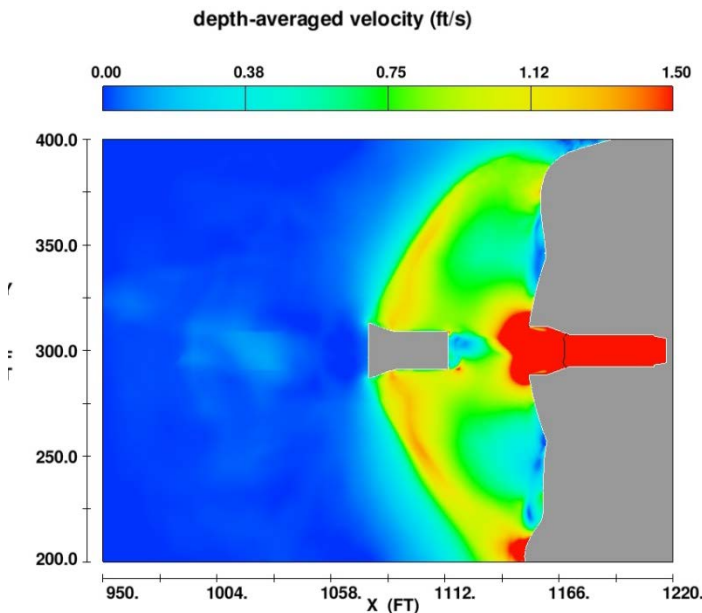


Figure 27. — Depth averaged velocities for the Gate-down simulation. X values represent project stationing.

The maximum depth simulation was achieved with the gate-up scenario using the middle intake #3. Simulations showed that the zone of influence for the intake was small, and flows further than 20 feet from the intake were strongly affected by general reservoir currents (Figure 28).

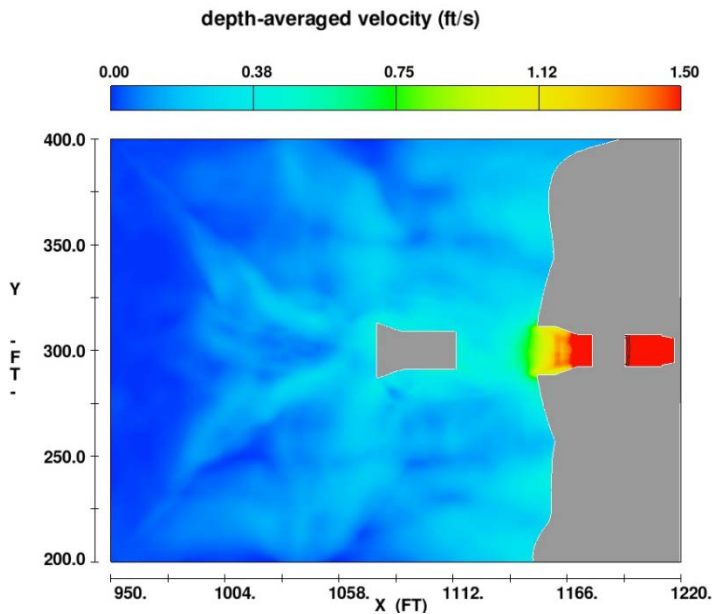


Figure 28. — Depth averaged velocities for the Gate-up simulation.

## Velocity gradients within the intake structure

Velocity gradients from the two extreme cases were compared to the extremes found in the interim flume results. To compare with the interim flume studies, the values for velocity and velocity gradient were extracted 2 feet below the reservoir surface. The velocity magnitude for the gate-down simulation is shown in Figure 29 and the velocity and velocity gradient chart is shown in Figure 30. These results were favorable since the velocity gradient did not exceed 0.4 ft/s/ft prior to the 8 ft/s capture velocity. The velocity magnitude for the gate-up simulation is shown in Figure 31 and the velocity and velocity gradient chart is shown in Figure 32. These results were also favorable since the velocity gradient did not exceed 1.0 ft/s/ft prior to the 8 ft/s capture velocity. However, the elevation for data extraction for the gate-up simulation crossed through the trashrack and grate support structure, causing the velocity output to be zero inside the beams, and the velocity gradient computation used that zero value. This caused dips in the resulting values.

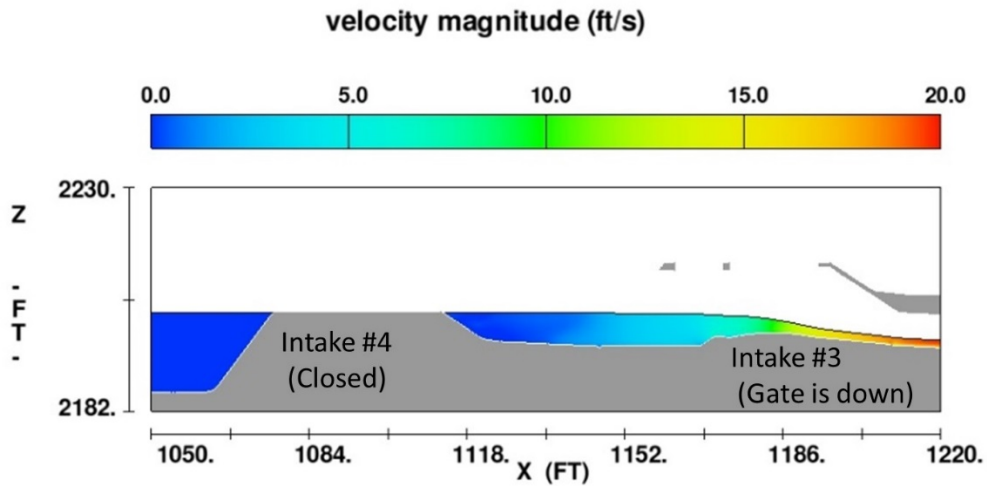


Figure 29. — Velocities for the gate-down simulation. The next-downstream inlet was modeled as a solid object (not containing an opening).

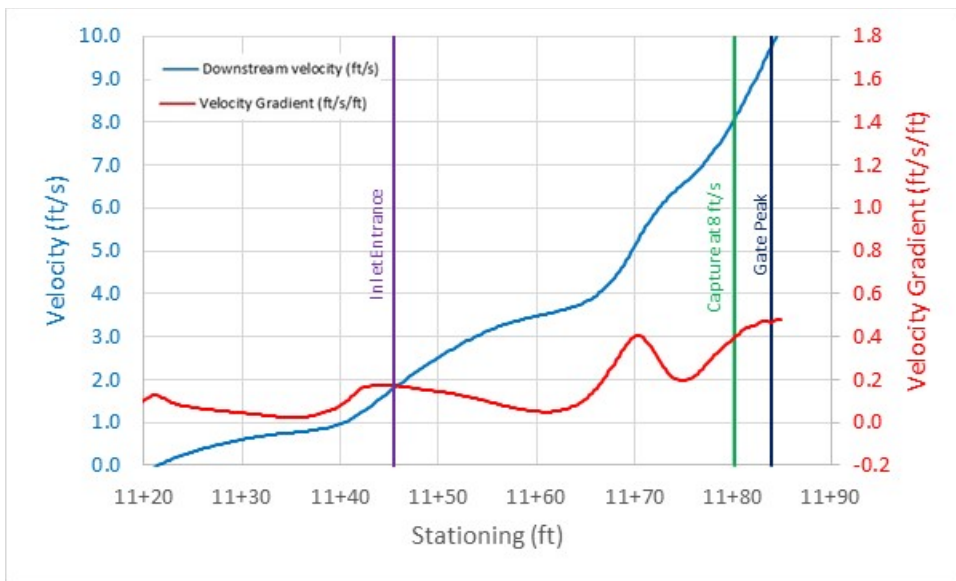


Figure 30. — Velocity and velocity gradient for the gate-down simulation.

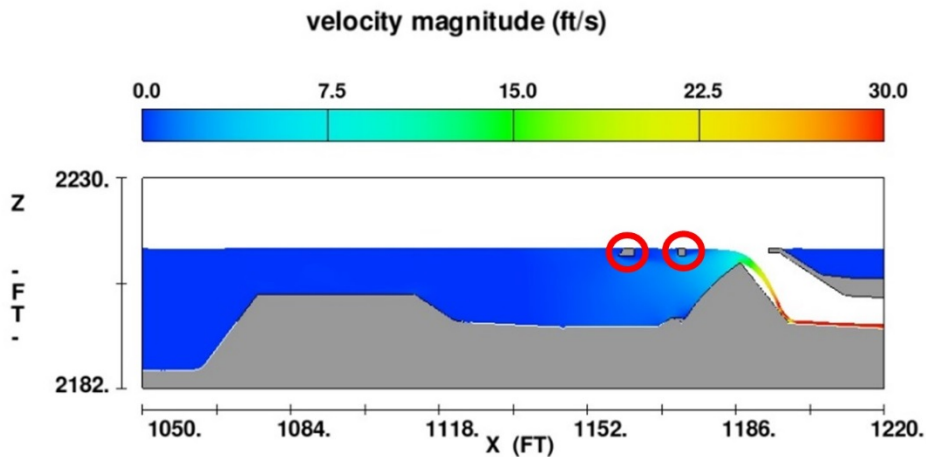


Figure 31 — Velocities for the Gate-up simulation. The trashrack and grate support structures circled in red interfere with calculation of velocity gradients in the plane that is 2 feet below the reservoir water surface, causing disruption of the flow field. The downstream inlet was modeled as a solid object (not containing an opening).

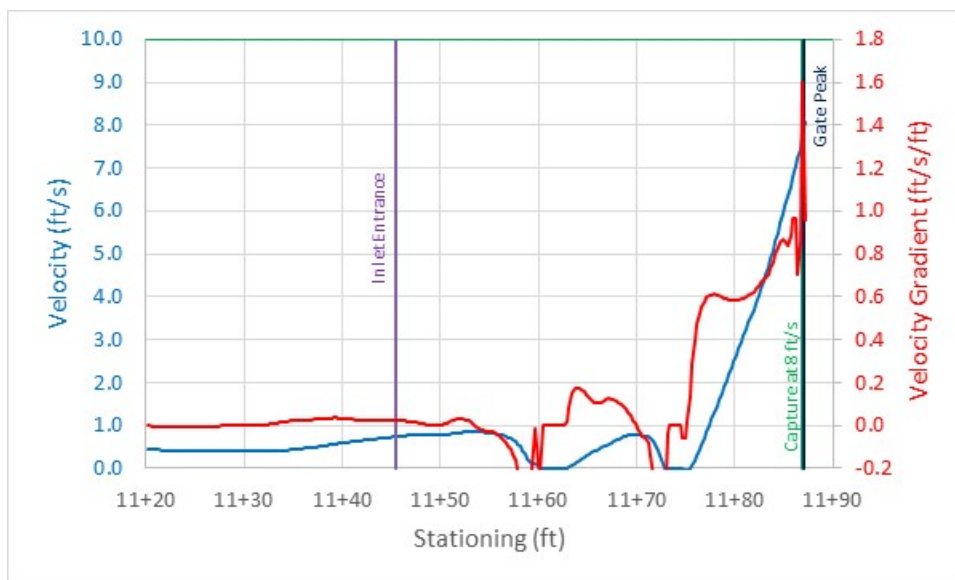


Figure 32. — Velocity and velocity gradient for the gate-up simulation. The capture velocity of 8 ft/s was achieved slightly upstream of the gate peak (lines appear to overlap). The elevation for data extraction for the gate-up simulation crossed through the trashrack and grate support structure (Figure 31), causing the velocity output to be zero, and the velocity gradient computation used that value.

## Flow conditions downstream of the ramp-weir

To minimize injury and disorientation to fish, the Design and Core teams determined it was necessary to design the system to be free of hydraulic jumps between the intake gate and the helix structure. A hydraulic jump is formed when the flow transitions from supercritical ( $Fr > 1$ ) to subcritical ( $Fr < 1$ ).

Accordingly, once the flow in the conduit reaches supercritical, as it does near the peak of the ramp-weir, the flow is required to stay supercritical to prevent a hydraulic jump. A Froude number, as defined above, greater than 1.0 is supercritical and can be used as a simple test to determine that a hydraulic jump will not form.

Several designs were tested to insure a hydraulic jump did not form. One significant change that helped assure this was changing the conduit between the intakes and helix from the original concept of 7 ft diameter pipe to the proposed 7 ft by 7 ft rectangular conduits. The 7 ft diameter pipe could have been used, but the conduits would need to be lowered, which would also lower the elevation of the helix structure. This would have caused additional excavation costs. A 51-foot long transition from the end of the ramp-weir to the 7 ft by 7 ft rectangular conduit was found to be beneficial in suppressing the height of standing waves.

Velocity, depth, and Froude number for the gate-down simulation is shown in Figure 33, and for the gate-up in Figure 34. Both simulation results demonstrated that the Froude number remains above 1 indicating that the flow is free of hydraulic jumps.

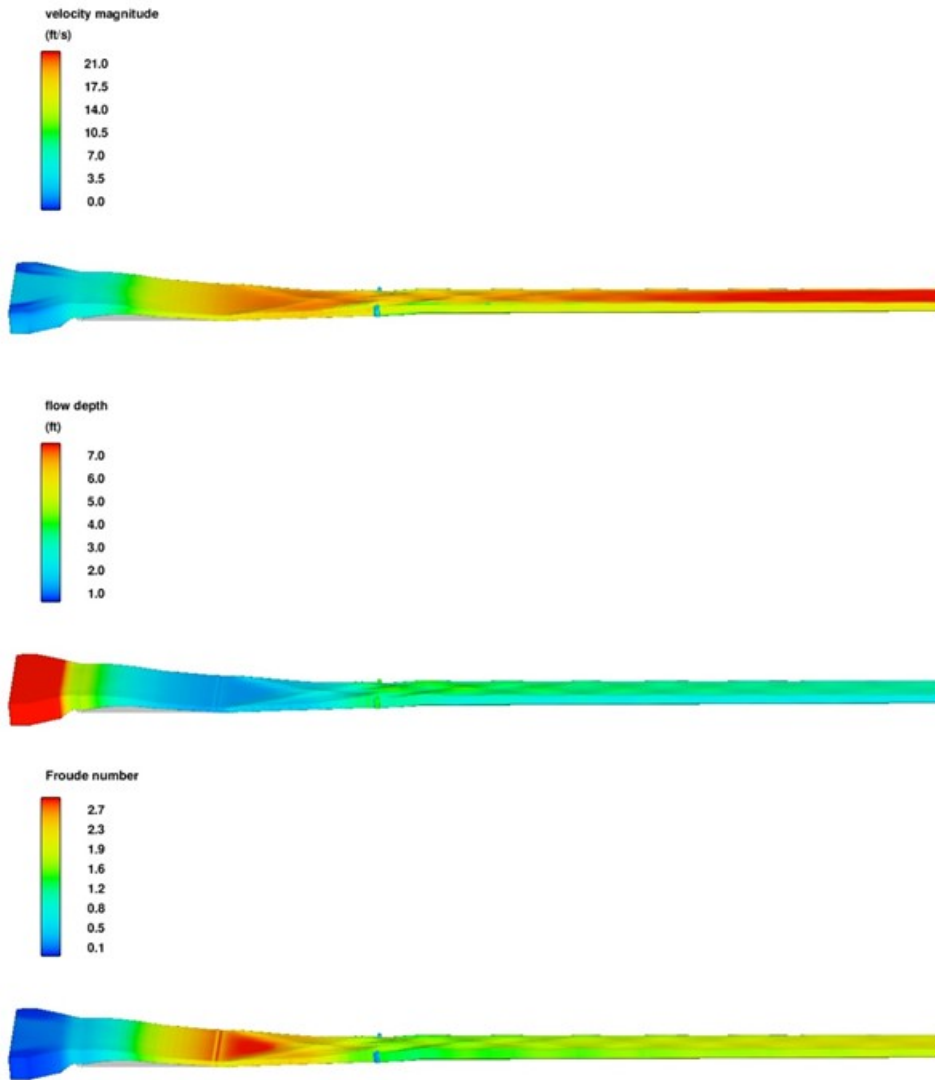


Figure 33. — Velocity magnitude, flow depth, and Froude number for the gate-down simulation. The gate object is shown in grey (very thin in the down position) and is arched. Once supercritical flow ( $Fr > 1$ ) is achieved, the flow remains supercritical indicating a hydraulic jump will not form. Standing waves were minor, less than 1 ft high.

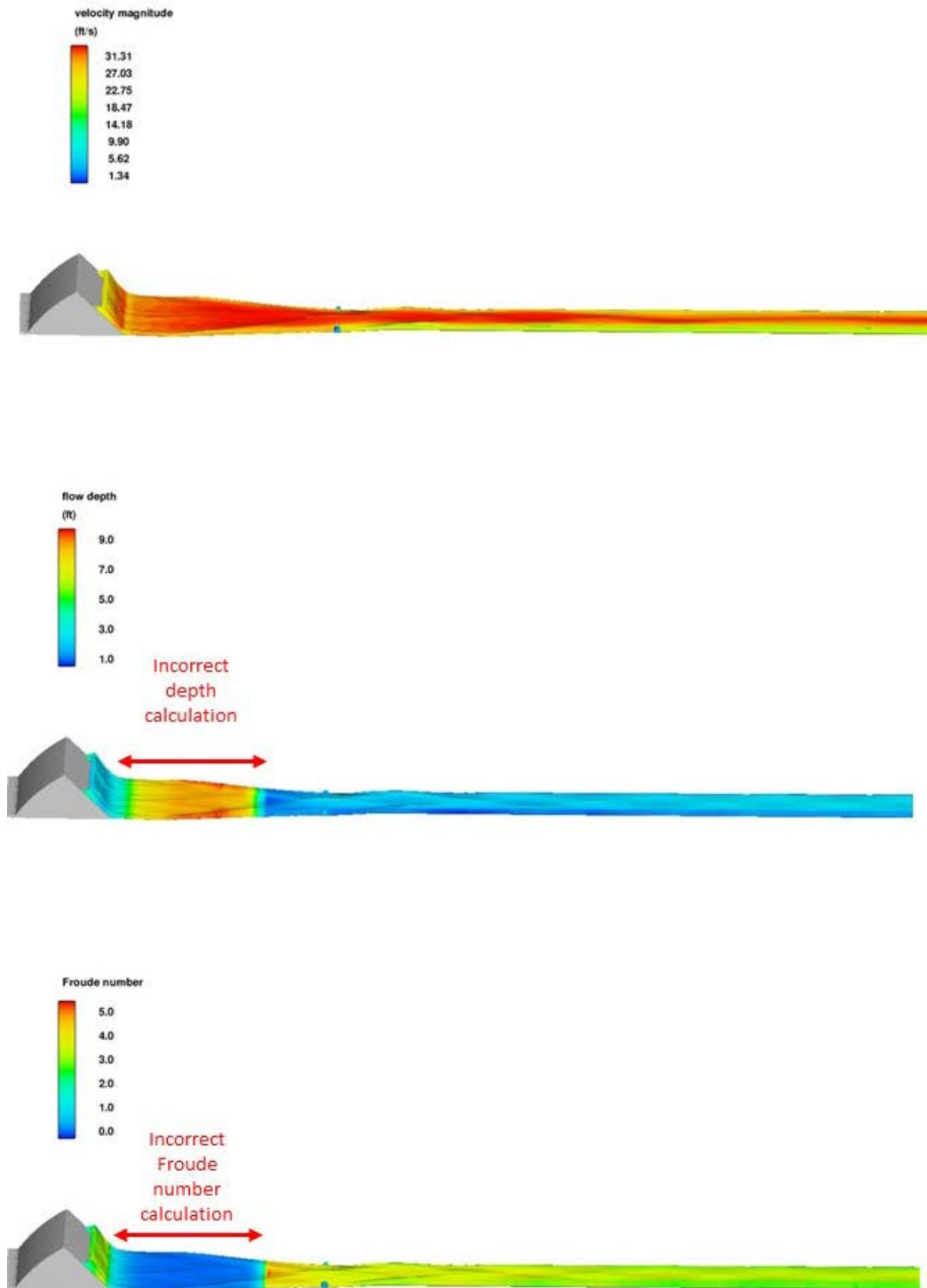


Figure 34. — Velocity magnitude, flow depth, and Froude number for the gate-up simulation. The gate object is shown in grey. Once supercritical flow ( $Fr > 1$ ) is achieved, the flow remains supercritical indicating a hydraulic jump will not form. Due to this portion of the intake being submerged at this reservoir water surface elevation (ft) as shown in Figure 28 and Figure 31, the depth and Froude number computation is not correct for the range indicated in red. Standing waves were minor, less than 1 ft high.

## Transition into the helix structure

Both the gate-down and gate-up simulation domains started in the reservoir and ended inside the helix structure. Approximately one quarter of a helix loop was included so the downstream boundary condition would not influence the flow as it enters the helix with a “sink” extending over the next half a loop (Figure 26) to remove helix flow. A small amount of standing water was found in the upstream helix loop.

The transition into the helix used a warped floor to avoid offsets at the edge of the helix as previously studied [1]. Due to changes in the design, the approach to the warped floor was increased in slope for this study.

For the simulated middle intake, only minor differences in velocity and depth were found based on gate position. The gate-down simulation showed the peak velocity around 27 ft/s and a maximum depth of 6.9 feet in the helix (Figure 35). The maximum depth in the warped floor section was 5.0 feet. The gate-up simulation showed peak velocity around 30 ft/s and a maximum depth of 7.0 feet in the helix (Figure 36). The maximum depth in the warped floor section was 4.4 feet.

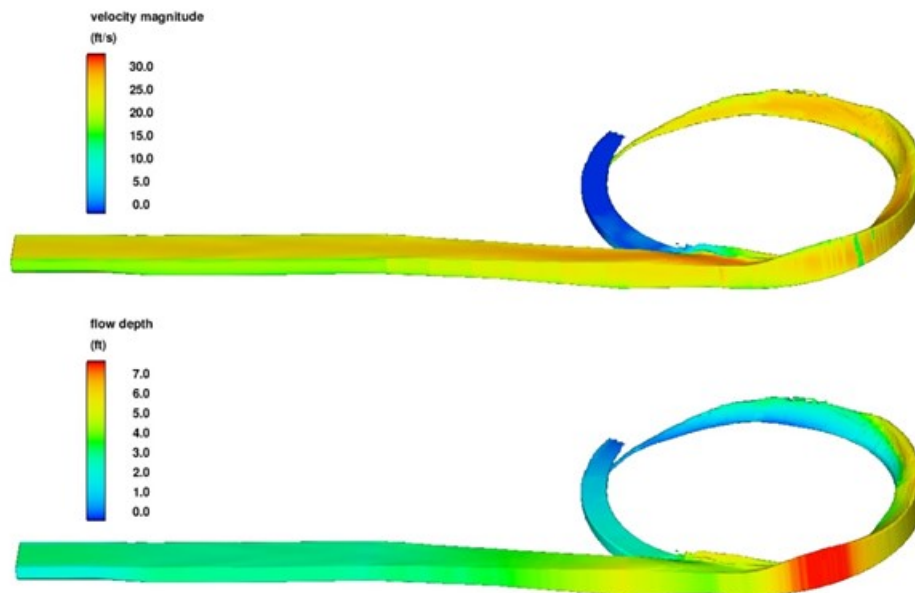


Figure 35. — Velocity and depth for the gate-down simulation.

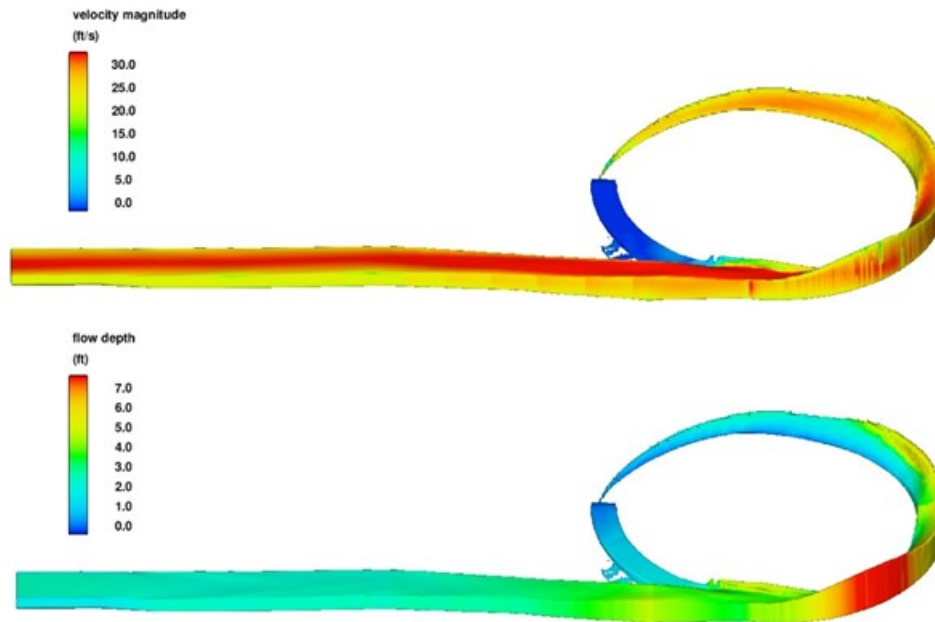


Figure 36. — Velocity and depth for the gate-up simulation.

## Conclusions

A coordinated series of CFD simulations and physical model tests was used to develop the design of the intake structures needed for the Cle Elum Dam downstream fish passage facility. Preliminary physical model tests considered inlet structures designed to maintain velocity gradients below 1 ft/s/ft, until new research suggested that much lower gradients would be needed for safe passage. When it appeared to be cost-prohibitive to fully satisfy the new velocity gradient requirements, the Core team directed that a subsequent series of CFD studies and physical model tests be used to evaluate the flow field associated with the successfully operating interim flume structure. Additional physical model studies were then used to evaluate design alternatives that would produce a more gradual acceleration of flow into the intake and shift the location of the velocity capture zone further upstream. Experience gained from all of these studies was then used to develop the final inlet configuration which utilizes a series of inlets at 10.5 ft elevation intervals, each inlet provided with an adjustable gate having upstream and downstream ramp sections and upstream training walls to provide gradual acceleration of flow into the inlet and maintain desirable flow conditions in the channels leading from inlet structures to the helical fish passage facility. The gradually increasing velocity gradient was considered by the Core team to be more effective for passing fish than a very low gradient that abruptly increased in

magnitude (potentially causing fish to retreat away from the structure). Thus, the overflow gate with upstream ramp and training walls to control flow into the inlet is an important component of the final design.

An equally important feature of the final design is the downstream ramp that extends downstream from the overflow crest, as illustrated in Figure 37. This feature reduces potential injury to fish by maintaining supercritical flow in the conduit leading into the helix and eliminating turbulence at the toe of the ramp-weir structure caused by the flow plunging over the crest. The downstream ramp will be designed so that the upstream edge will move with the overflow crest, while the downstream edge slides along the surface of the channel floor.

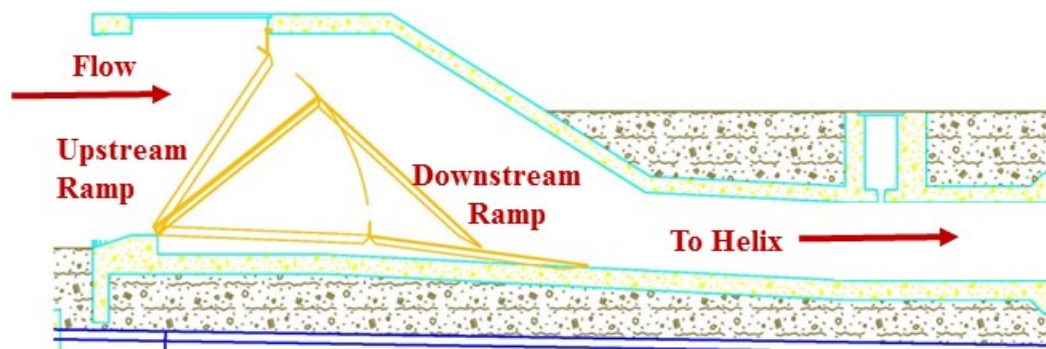


Figure 37. — Schematic of final configuration for inlet gate, utilizing an Obermeyer gate to provide an adjustable ramp-weir height. The Obermeyer gate has an attached downstream ramp to maintain supercritical flow.

# References

1. Hanna, Leslie J., Higgs, Jim, Mefford, B., Wagner, J. (2015). “Helix Design for Downstream Fish Passage at Cle Elum Dam”, U.S. Bureau of Reclamation, Hydraulic Laboratory Report, HL-2015-01
2. Bureau of Reclamation (2011). *Final Planning Report Cle Elum Dam Fish Passage Facilities*, United States Department of the Interior, Bureau of Reclamation, Pacific Northwest Region Columbia-Cascades Area Office Yakima, Washington
- 3 Bureau of Reclamation (2005). “Phase I Assessment Report Storage dam Fish Passage Study”, Yakima Project, Washington, Technical Series No. PN-YDFP-001, 2003, rev. 2005.
4. Bureau of Reclamation, “Cle Elum Dam Interim Fish Passage Operations ‘2006-2009’ Annual Reports”, Technical Series No. PN-YDFP-‘011-015’, 2006 through 2009.

# Appendix A – Description of CFD Modeling

## FLOW-3D

This study used the commercially available Computational Fluid Dynamics program FLOW-3D Version 10.1.1.05 by Flow Science Inc. <sup>1</sup>, which is a finite difference, free surface, transient flow modeling system that was developed from the Navier-Stokes equations, using up to three spatial dimensions.

The finite difference equations are based on a fixed Eulerian mesh of non-uniform rectangular control volumes using the Fractional Area/Volume (FAVOR) method<sup>2</sup>. Free surfaces and material interfaces are defined by a fractional volume-of-fluid (VOF) function. FLOW-3D<sup>®</sup> uses an orthogonal coordinate system as opposed to a body-fitted system.

The results from FLOW-3D simulations were analyzed to identify, quantify, and qualify the key hydraulic characteristics.

## Simulation Assumptions

The following assumptions were made and options selected for each simulation:

- One fluid (air simulated with void space)
- Free surface
- Cubed cell volumes (length, width, and height of each cell were equal) to reduce numerical errors
- Turbulence model: Renormalized Group (RNG) model with Dynamically computed Maximum Turbulent Mixing Length
- Pressure Solver: Generalized Minimal Residual (GMRES)
- Water at 20° Celsius (68° degree Fahrenheit)
  - Water density of 1.9403 slugs/ft<sup>3</sup>
  - Dynamic viscosity of  $2.08855 \times 10^{-5}$  lbf-s/ft<sup>2</sup>
  - Incompressible
  - Water from the withdrawal zone (top 10 feet) has been described as warm

---

<sup>1</sup> Flow Science Inc., Introduction to FLOW-3D, 1996.

<sup>2</sup> J.M. Sicilian, "A FAVOR Based Moving Obstacle Treatment for FLOW-3D," Flow Science, Inc. Technical Note #24, April 1990 (FSI-90-TN24).

- Volume of Fluid Advection: Automatic fluid convection
- Momentum Advection: First Order
- Convergence controls: Default values were used
- Gravity:  $-32.2 \text{ ft/s}^2$  in the vertical (Z) direction

## **Solids model development**

Structural objects used stereolithography files that were generated using commercially available AutoCAD 2014 and imported into FLOW-3D.

Topography was converted from a point file to stereolithography using an in-house FORTRAN program.

# Appendix B

## Inlet Transitions – Velocity Gradient Criteria 1.0 ft/s/ft

Based on discussions with the Cle Elum Core team, the initial concept for the intake structure was based on a maximum approach velocity gradient of 1.0 ft/s/ft until a capture velocity of 8 ft/s was reached. The intake structure consisted of six separate inlets following the bank line within the reservoir, each with a vertical intake zone of about 10 ft (Figure B-1). Flow into the structure for this configuration would be controlled by a fish-friendly valve such as the pinch valve shown Figure B-2. The initial design for the inlet entrance section from the reservoir used a bell mouth shape to allow gradually accelerating flow to be pulled from the reservoir over an operating range of 200 ft<sup>3</sup>/s to 400 ft<sup>3</sup>/s, so that the velocity gradient into the structure would not exceed the stated criteria (Figure B-3 and Figure B-4).

The initial design concept was to be able to have two inlets operating at one time, and the two inlet flows would converge inside of the helix structure. As such it was necessary to physically model three inlets, since the flow to the lower operating inlet would be influenced by the next lower inlet. For single inlet flows, only the middle model inlet was tested since the inlet above was outside of the zone of flow influence. In each case presented, results caused changes that were made to the model prior to testing the lowest inlet which would have been used to model the lowest prototype inlet. For single inlet flows, the middle model inlet would properly model the top five inlets.

These three of the six inlets for the initial design concept were constructed on a 1:9.5 scale in the Denver laboratory, since this was all that was necessary to represent the performance of the structure (Figure B-5). For initial testing, surrounding topography was not installed so that modifications to the structure could easily be made. Figure B-6 shows velocities approaching the middle model inlet for a flow rate of 400 ft<sup>3</sup>/s, measured 2 ft below the water surface at the inlet centerline. The figure shows that velocities approaching the inlet reach capture velocity just before flow enters into the downstream pipe transition section. However, there are standing waves and turbulence that extend upstream from the pipe transition that may cause fish to retreat away from the structure before

capture velocity is reached (Figure B-7). As a result, this configuration was considered unacceptable.

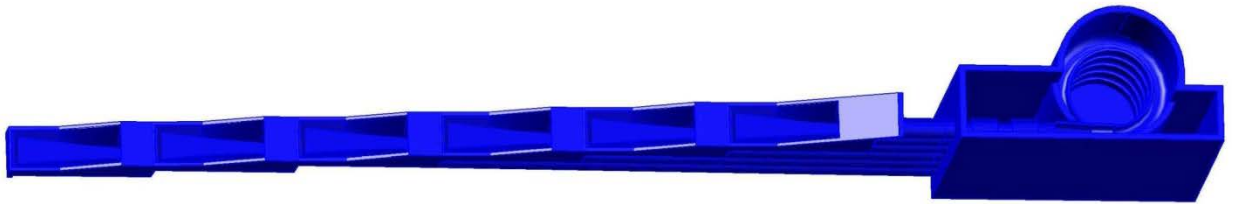


Figure B-1. — Initial concept for intake structure design following bank line.



Figure B-2. — Pinch valve used to control flow into initial intake structure design.



Figure B-3. — Initial design concept for individual inlets for intake structure.

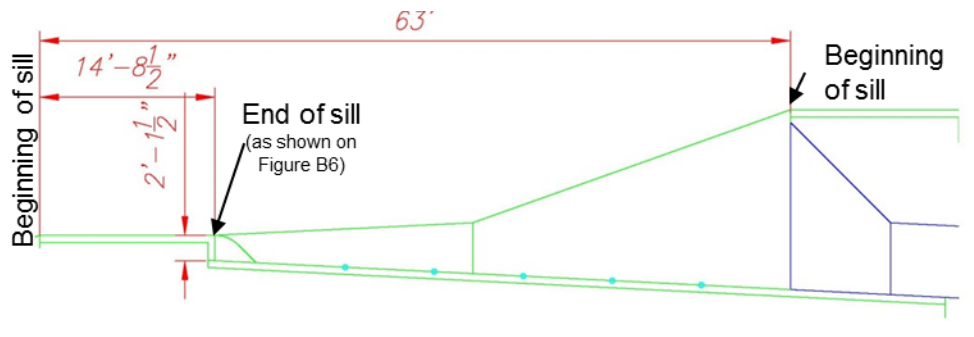


Figure B-4. — Centerline profile view for initial design of individual inlets for intake structure



Figure B-5. — Only three of the six inlets are used to represent the intake structure in the physical model. Adjacent reservoir topography was not included for the initial model runs.

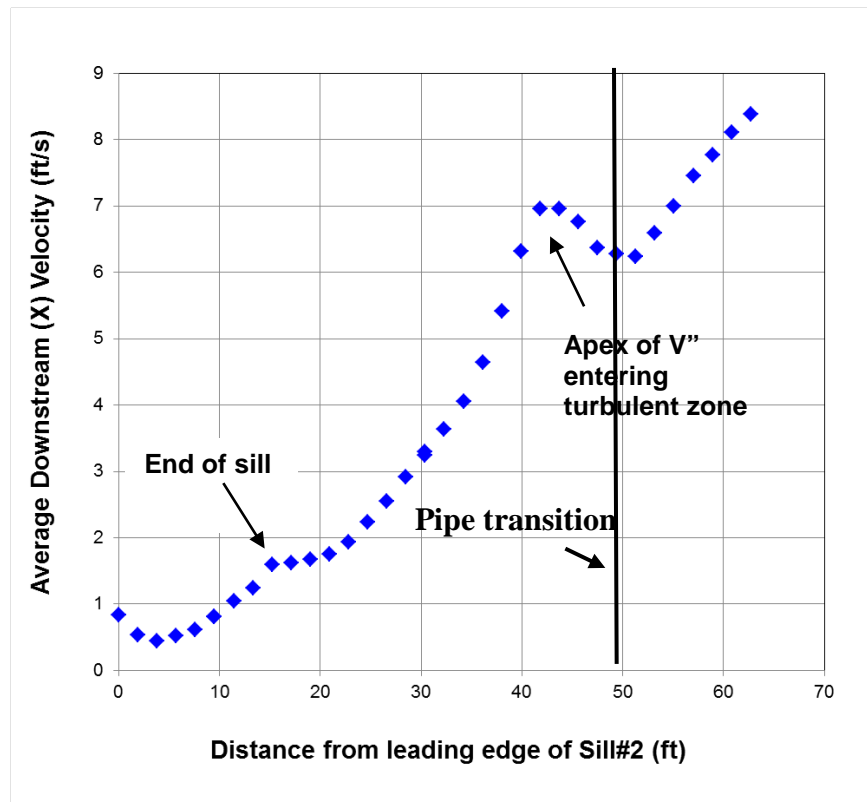


Figure B-6. — Average velocities approaching the inlet for a flow rate of 400 ft<sup>3</sup>/s, measured 2 ft below the water surface at the inlet centerline. See figure B-3 for “End of sill” location.

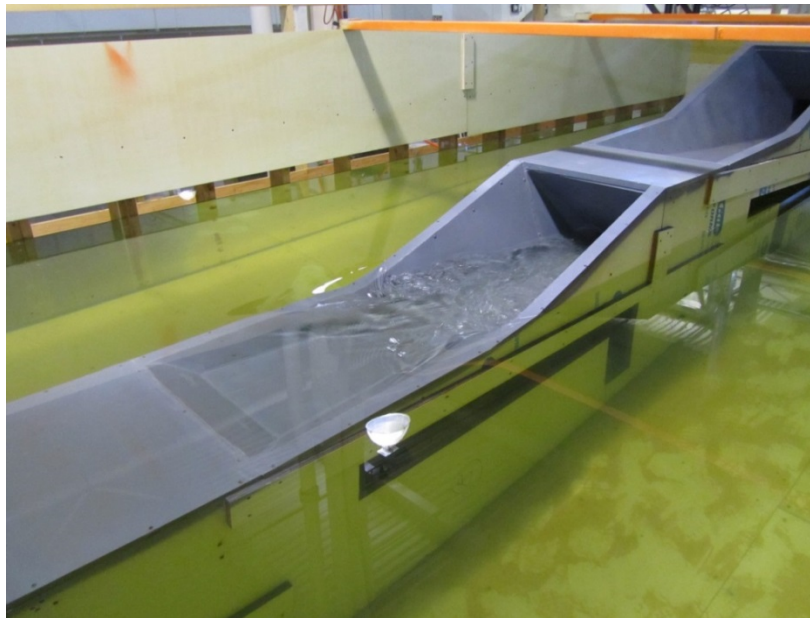


Figure B-7. — Standing waves and turbulence at inlet show undesirable entrance conditions.

The inlet was modified to provide smoother acceleration into the structure by installing a constant slope from the downstream edge of the inlet sill and sidewalls down to the inlet floor (Figure B-8). The modified structure (described as the T3 transition) was tested with a flow rate of 400 ft<sup>3</sup>/s (Figure B-9). This time, capture velocity was reached just prior to entering the turbulent zone (as indicated by the location of the apex of the “V”), as shown in Figure B-10. However velocity drops below capture velocity again after entering an area of turbulence before entering the pipe. The “V” apex location, identified on each graph, is the farthest downstream point before flow enters a zone of turbulence or standing waves; for the purposes of this report. Looking at velocity gradient in Figure B-11, the velocity gradient remains well below the original criteria of 1 ft/s/ft until capture velocity is reached, and therefore remains within the stated criteria.

Figure B-12 shows the T3 inlet transition operating at 200 ft<sup>3</sup>/s. This time capture velocity is reached well before it enters the pipe and velocity continues to increase. Velocity gradient for this flow condition remains below 1 ft/s/ft until capture velocity is reached and therefore remains within the stated criteria.

Next, testing was conducted with the same two flow rates, only this time the reservoir was set to a higher elevation with respect to the entrance pipe elevation. With the higher head condition (2.62 ft and 5.54 ft depth above the inlet sill for 200 ft<sup>3</sup>/s and 400 ft<sup>3</sup>/s respectively) the downstream valve had to be throttled to maintain the same flow rates (Figure B-15 and Figure B-16). As a result, although flow at the entrance became smoother and velocity gradients stayed well within criteria, capture velocity is never reached (Figures B-17 through B-20). This meant that the potential for fish retreating away from the structure was much more likely since they would reach a turbulent or dark zone (entering the pipe) before capture velocity was reached. As a result of these findings, the T3 transition design was also considered unacceptable. At this point physical testing was discontinued due to the introduction of new velocity gradient criteria, and subsequent CFD work was focused on intake designs utilizing a vertical weir or inclined ramp-weir for flow control.



Figure B-8. — Inlet is modified into the T3 transition.

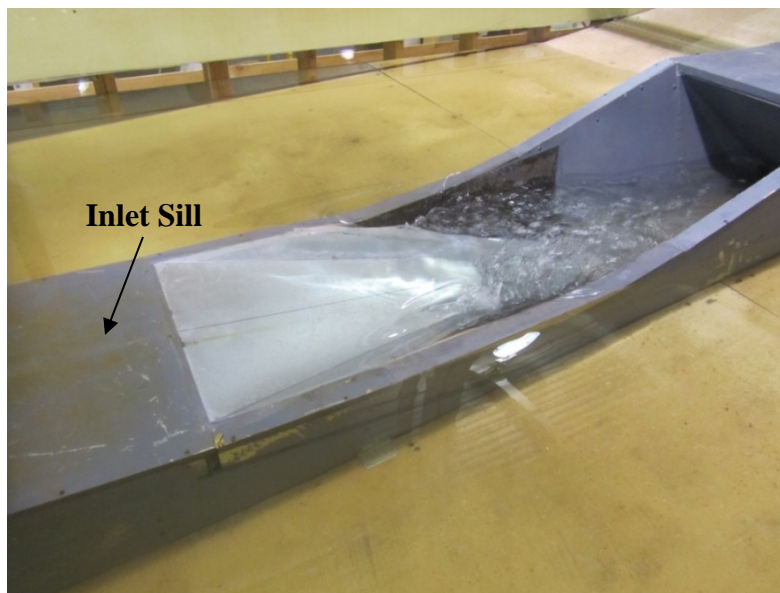


Figure B-9. — Transition T3 inlet operating at 400 ft<sup>3</sup>/s with an inlet sill depth of 3.5 ft.

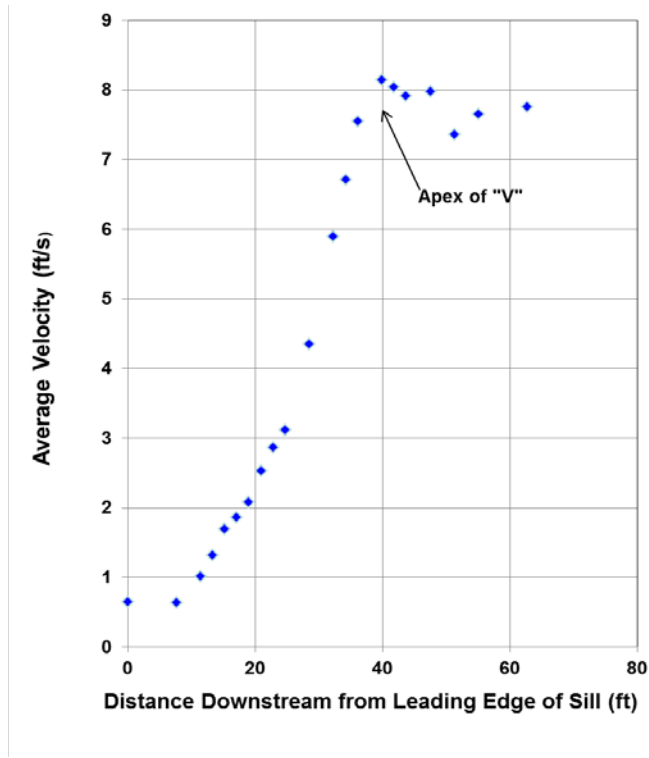


Figure B-10. — Average velocities measured approaching and within the T3 transition inlet while operating at 400 ft<sup>3</sup>/s with a sill depth of 3.5 ft.

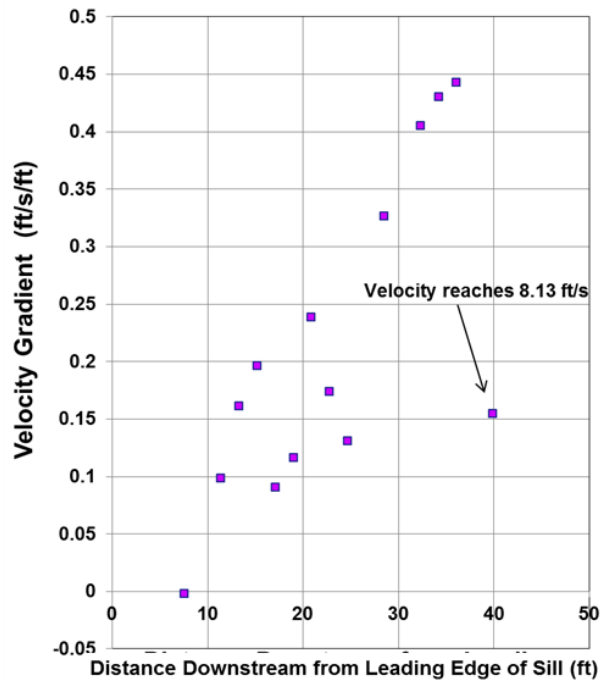


Figure B-11. — Velocity gradient measured approaching and within the T3 transition inlet while operating at 400 ft<sup>3</sup>/s with a sill depth of 3.5 ft.

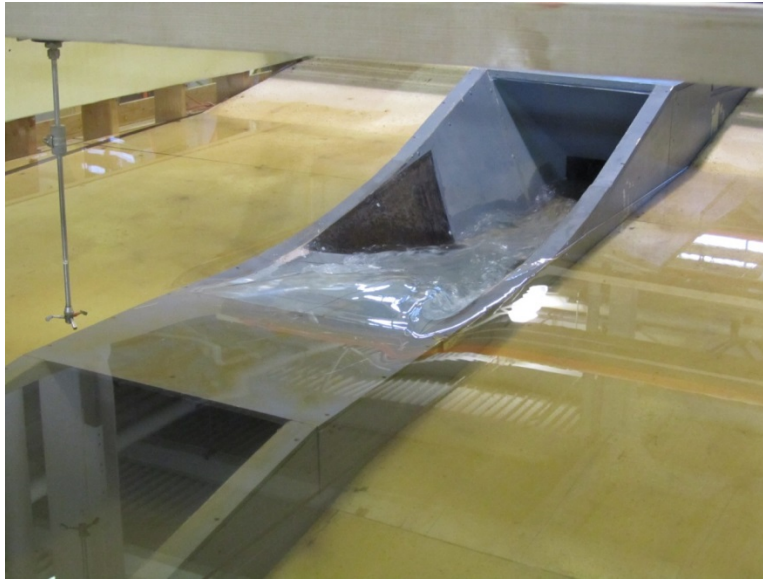


Figure B-12. — T3 transition inlet operating at 200 ft<sup>3</sup>/s with a sill depth of 1.98 ft.

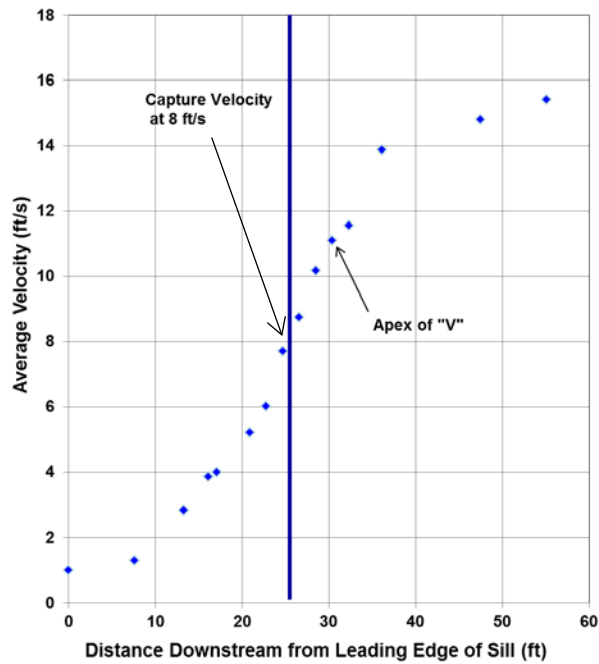


Figure B-13. — Average velocities measured approaching and within the T3 transition inlet while operating at 200 ft<sup>3</sup>/s with a sill depth of 1.98 ft.

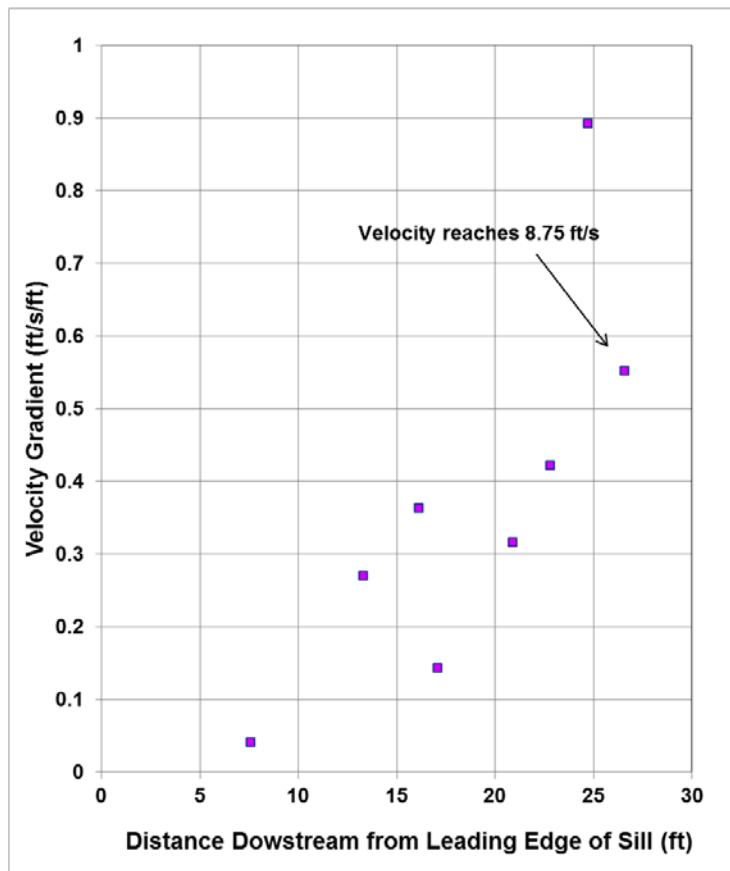


Figure B-14. — Velocity gradient measured approaching and within the T3 transition inlet while operating at 200 ft<sup>3</sup>/s with a sill depth of 1.98 ft

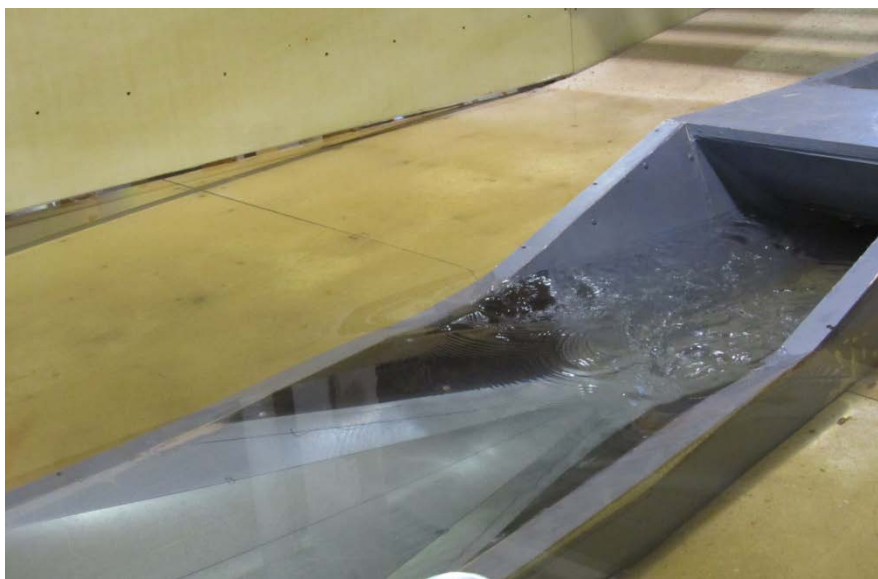


Figure B-15. — T3 transition inlet operating at 400 ft<sup>3</sup>/s with a sill depth of 5.54 ft.

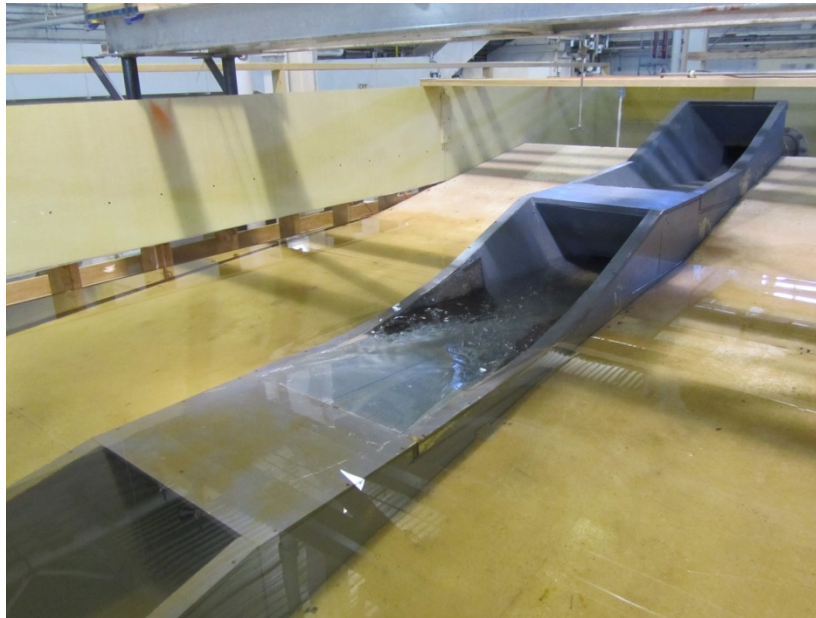


Figure B-16. — T3 transition inlet operating at 200 ft<sup>3</sup>/s with a sill depth of 2.62 ft.

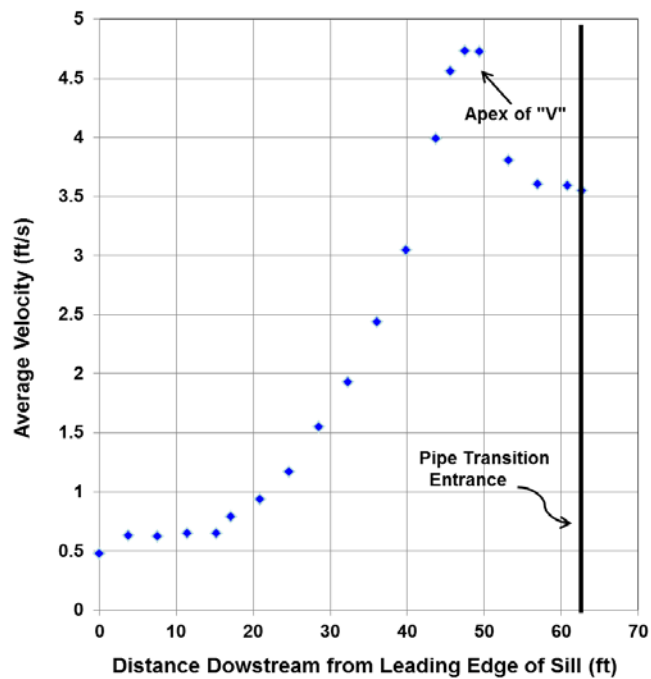


Figure B-17. — Average velocities measured approaching and within the T3 transition inlet while operating at 400 ft<sup>3</sup>/s with a sill depth of 5.54 ft.

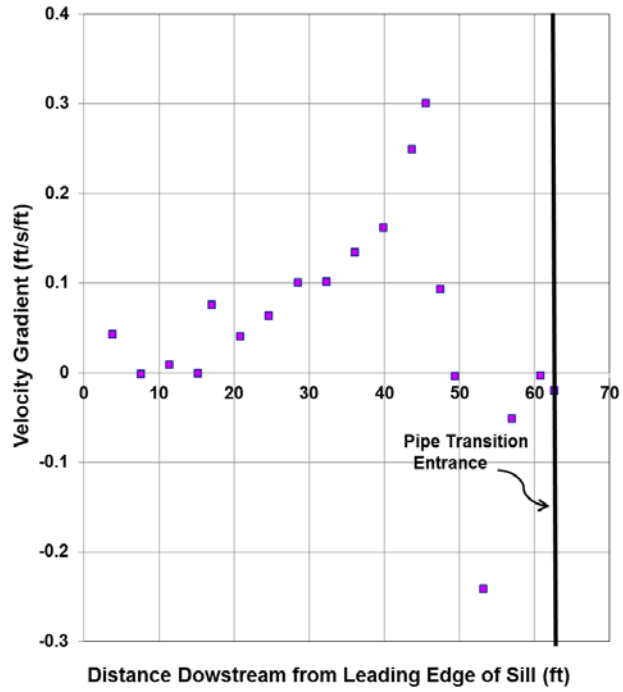


Figure B-18. — Velocity gradient measured approaching and within the T3 transition inlet while operating at 400 ft<sup>3</sup>/s with a sill depth of 5.54 ft.

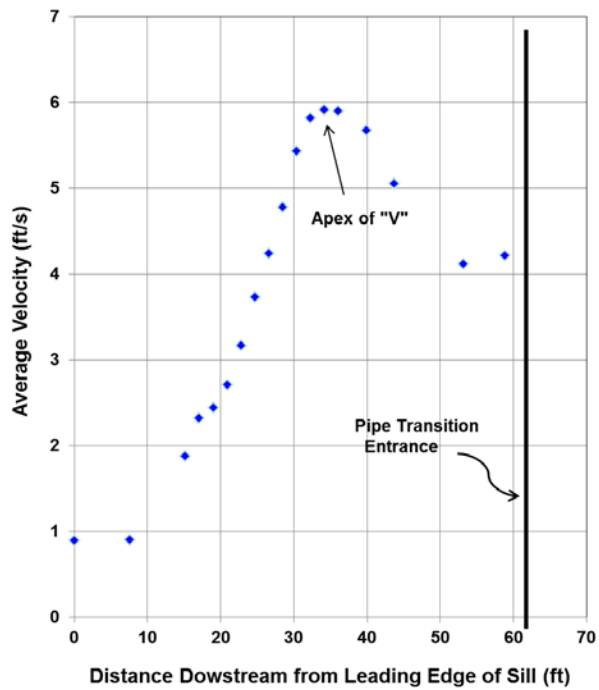


Figure B-19. — Average velocities measured approaching and within the T3 transition inlet while operating at 200 ft<sup>3</sup>/s with a sill depth of 2.62 ft.

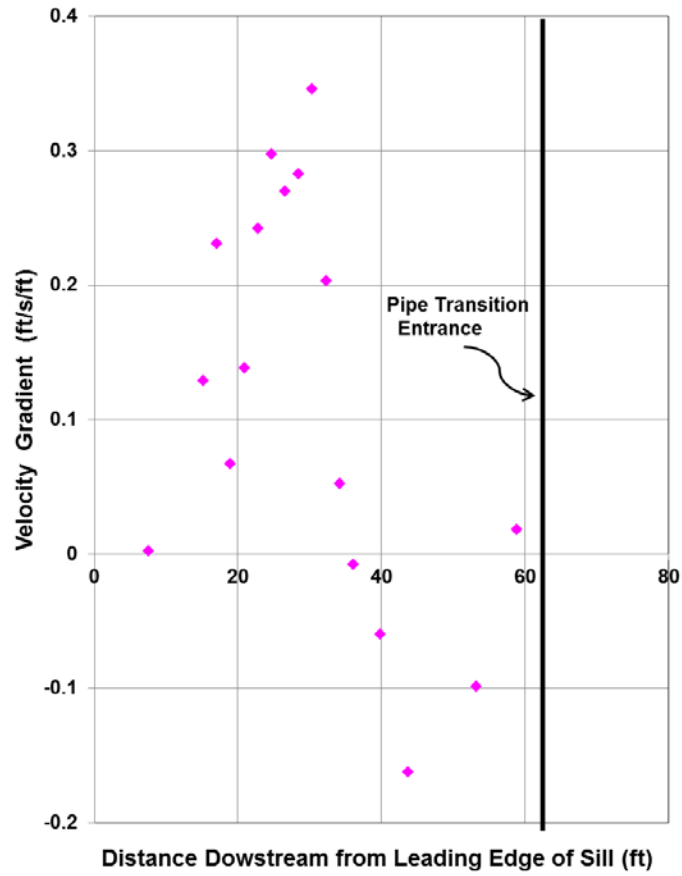


Figure B-20. — Velocity gradient measured approaching and within the T3 transition inlet while operating at 200 ft<sup>3</sup>/s with a sill depth of 2.62 ft.

# Appendix C

## Weir and Ramp-Weir Tests

Once the flow conditions entering the interim flume were well understood, testing was performed to develop an intake design that could be applied to each of the multi-level intakes needed for the helix structure. Tests were conducted with several weir heights, in both a vertical weir configuration similar to the stoplog weir entrance to the interim flume and with an upstream ramp attached to each weir (ramp-weir configuration) to determine the effect of a ramp on the intake velocity field and velocity gradients (Table C-1). The tests were conducted with a weir that spanned the 17 ft width of the originally proposed design inlet structure trough, since this configuration was readily available (Appendix B). In addition, side walls were added to the inlet trough section to prevent side-weir overflow. Training walls upstream from the weir crest (like those in the final inlet configuration) were not included in this series of tests.

For these test cases, it was also demonstrated that a fish-friendly control valve could be used to throttle flow to provide a tailwater pool below the weir to cushion fish dropping over the weir for any weir or ramp-weir configuration tested, as shown in Figure C-1. The additional tailwater depth prevents the jet flowing over the weir from immediately sweeping downstream. Instead, the jet energy is partially dissipated in a submerged hydraulic jump created by the additional tailwater depth.

Table C-1. Weir and ramp-weir combinations tested

Test Case #	Weir Height (ft)	Flow Rate (ft <sup>3</sup> /s)	Configuration
1	5.5	400	Vertical Weir
2	5.5	200	Vertical Weir
3	2.375	400	Vertical Weir
4	2.375	200	Vertical Weir
5	0.0	400	Vertical Weir
6	0.0	300	Vertical Weir
7	5.5	400	Ramp-Weir
8	5.5	200	Ramp-Weir
9	2.375	400	Ramp-Weir
10	2.375	200	Ramp-Weir



Figure C-1. — The same flow with (left) and without (right) control valve throttling to provide cushioned drop. Flow at 200 ft<sup>3</sup>/s over 2.375 ft high ramp weir (Test Case #10). The throttling effect can be used for any weir or ramp-weir configuration.

### Vertical Weir Tests

Weir heights of 5.5 ft, 2.375 and 0.0 ft were tested with intake flow rates of 400 ft<sup>3</sup>/s and 200 ft<sup>3</sup>/s. Tests at 400 ft<sup>3</sup>/s were conducted with approximately 4 ft of head above the weir crest, and tests at 200 ft<sup>3</sup>/s were conducted with approximately 2.5 ft of head above the weir crest. Figure C-2 shows the 5.5 ft weir operating at a flow of 400 ft<sup>3</sup>/s and 200 ft<sup>3</sup>/s with depths over the weir of 3.86 ft and 2.47 ft, respectively. Figure C-3 shows the 2.375 ft weir operating at a flow of 400 ft<sup>3</sup>/s and 200 ft<sup>3</sup>/s with depths over the weir of 3.96 ft and 2.37 ft, respectively. Figure C-4 shows the 0.0 ft weir operating at a flow of 400 ft<sup>3</sup>/s and 200 ft<sup>3</sup>/s with depths over the weir (inlet sill) of 4.45 ft and 2.87 ft, respectively. Figures C-5 through C-16 show the velocities and velocity gradients for each of these configurations.

The figures demonstrate that for each weir test, capture velocity is reached just as flow goes over the weir for all weir heights and flow rates. In each case, the 8 ft/s capture velocity occurred downstream of the weir, while velocity gradient upstream of the weir remained below the original 1.0 ft/s/ft criteria. For the 5.5 ft and 2.375 ft weirs, at 200 ft<sup>3</sup>/s, velocity gradient remains below 0.2 ft/s/ft until it is within 2-3 ft upstream from the weir. For a flow of 400 ft<sup>3</sup>/s, velocity gradient remains below 0.2 ft/s/ft until reaching a distance within 5 ft upstream from the weir. The 8 ft/s capture velocity which occurred downstream of the weir was deemed unfavorable to the team, since fish have the opportunity to return to the reservoir before going over the weir.

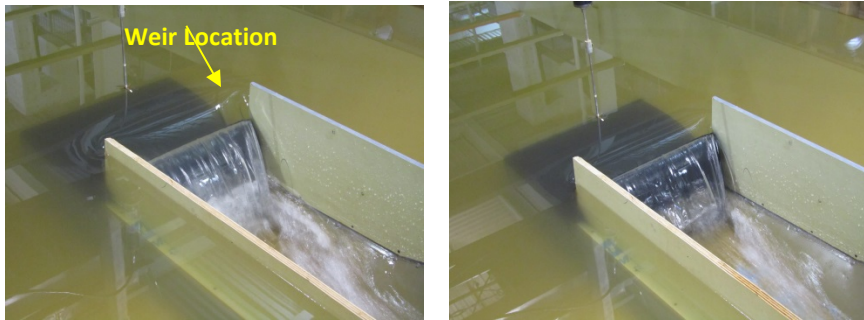


Figure C-2. — Vertical weir height 5.5 ft operating at 400 ft<sup>3</sup>/s (left) and 200 ft<sup>3</sup>/s (right) with depth over the weir at 3.86 ft and 2.47 ft respectively.



Figure C-3. — Vertical weir height 2.375 ft operating at 400 ft<sup>3</sup>/s (left) and 200 ft<sup>3</sup>/s (right) with depth over the weir at 3.96 ft and 2.37 ft respectively.

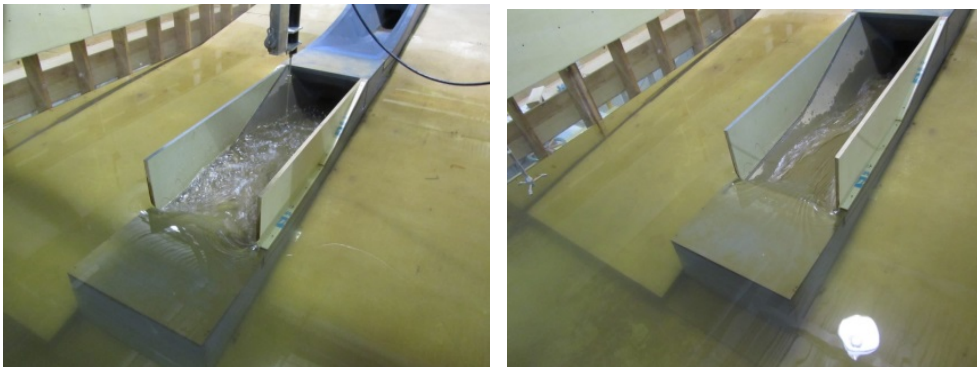


Figure C-4. — Weir height 0.0 ft operating at 400 ft<sup>3</sup>/s (left) and 200 ft<sup>3</sup>/s (right) with depth over the weir or inlet sill at 4.45 ft and 2.87 ft respectively.

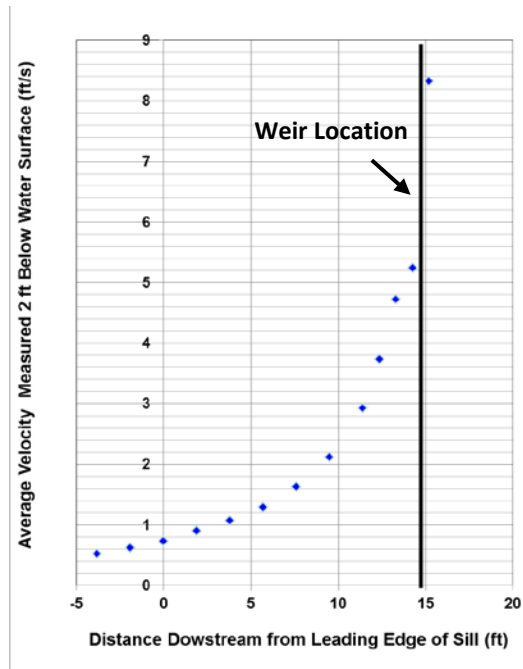


Figure C-5. — Average velocity measured 2 ft below the water surface approaching the 5.5 ft weir, operating at 400 ft<sup>3</sup>/s with a weir depth of 3.86 ft.

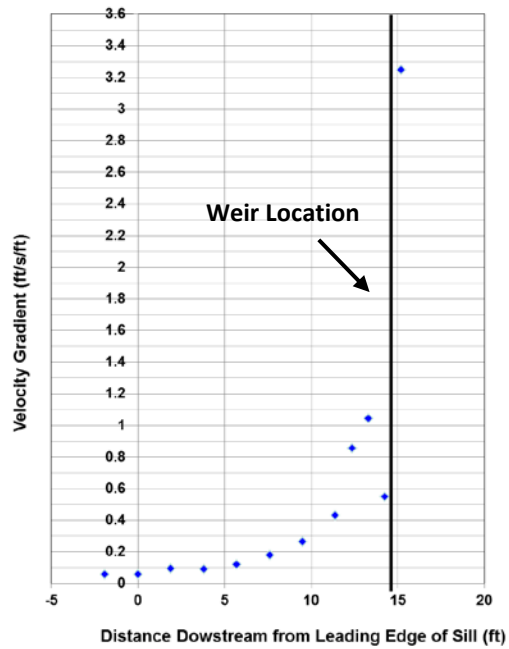


Figure C-6. — Velocity gradient measured 2 ft below the water surface approaching the 5.5 ft weir, operating at 400 ft<sup>3</sup>/s with a weir depth of 3.86 ft.

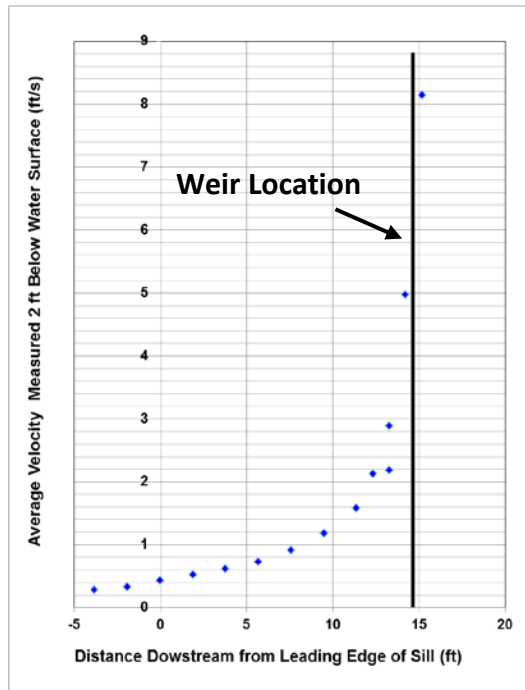


Figure C-7. — Average velocity measured 2 ft below the water surface approaching the 5.5 ft weir, operating at 200 ft<sup>3</sup>/s with a weir depth of 2.47 ft.

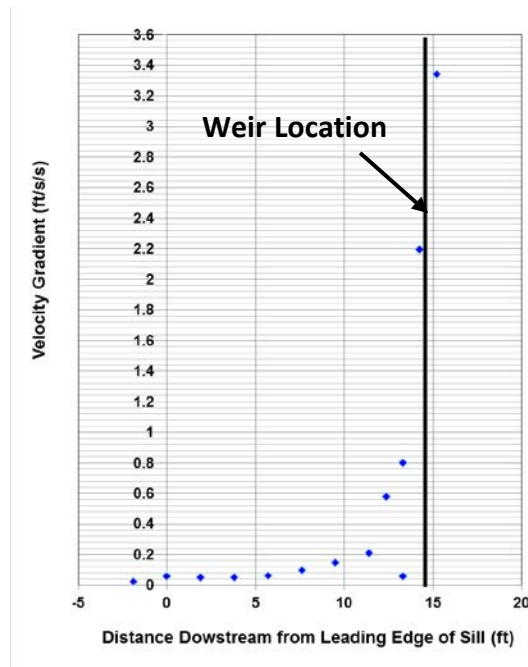


Figure C-8. — Velocity gradient measured 2 ft below the water surface approaching the 5.5 ft weir, operating at 200 ft<sup>3</sup>/s with a weir depth of 2.47 ft.

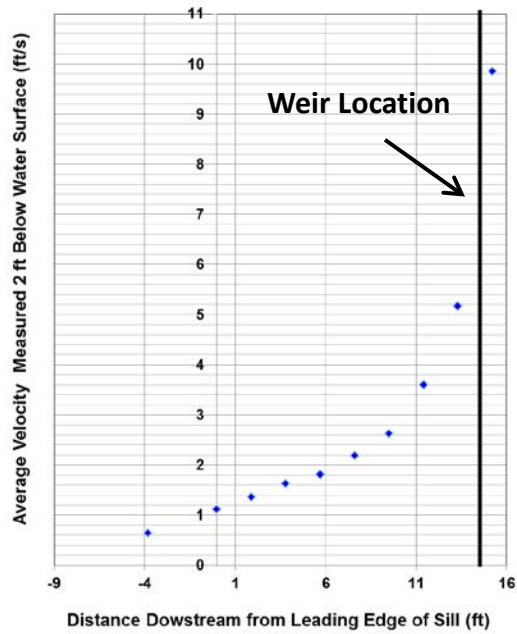


Figure C-9. — Average velocity measured 2 ft below the water surface approaching the 2.375 ft weir, operating at 400 ft<sup>3</sup>/s with a weir depth of 3.96 ft.

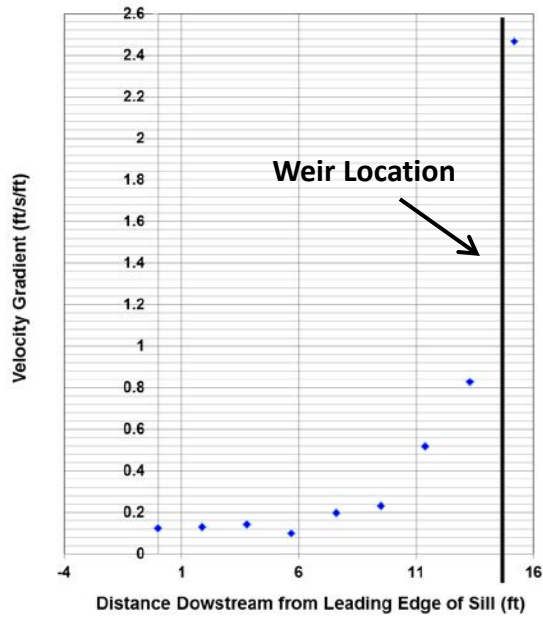


Figure C-10. — Velocity gradient measured 2 ft below the water surface approaching the 2.375 ft weir, operating at 400 ft<sup>3</sup>/s with a weir depth of 3.96 ft.

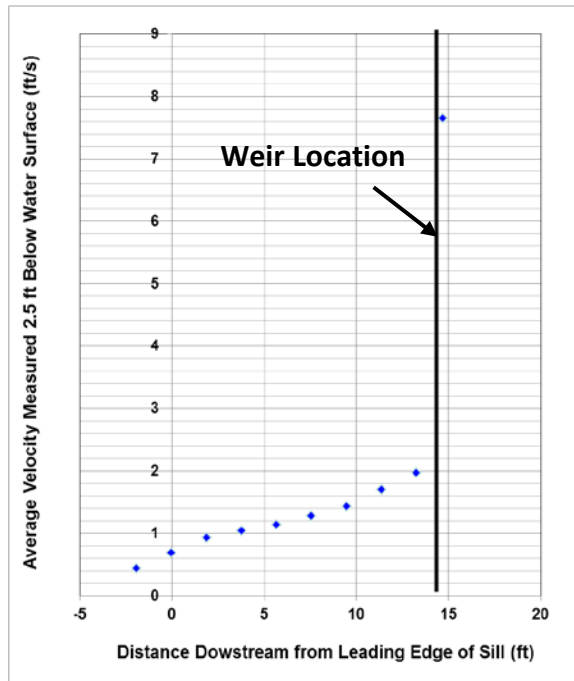


Figure C-11. — Average velocity measured 2 ft below the water surface approaching the 2.375 ft weir, operating at  $200 \text{ ft}^3/\text{s}$  with a weir depth of 2.37 ft.

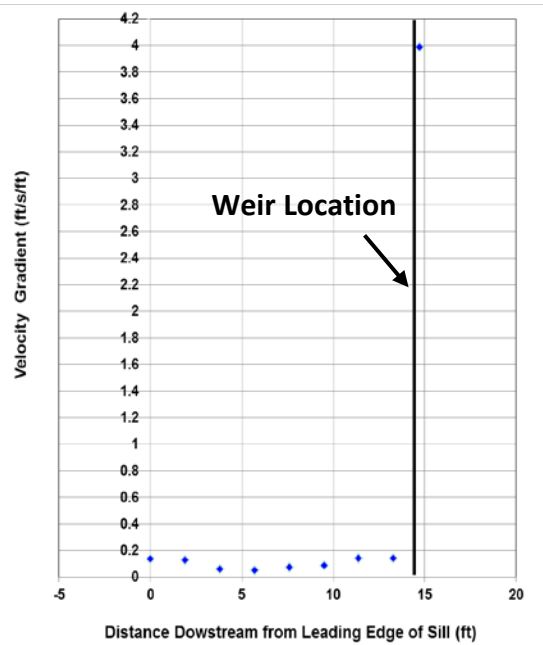


Figure C-12. — Velocity gradient measured 2 ft below the water surface approaching the 2.375 ft weir, operating at  $200 \text{ ft}^3/\text{s}$  with a weir depth of 2.37 ft.

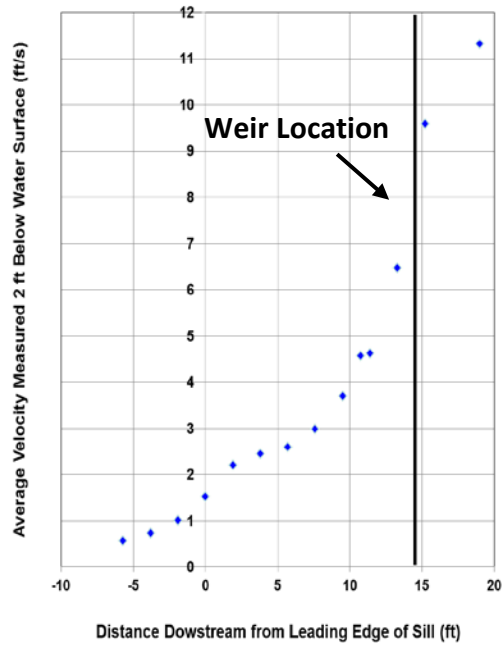


Figure C-13. — Average velocity measured 2 ft below the water surface approaching the 0.0 ft weir, operating at 400 ft<sup>3</sup>/s with a weir depth of 4.45 ft.

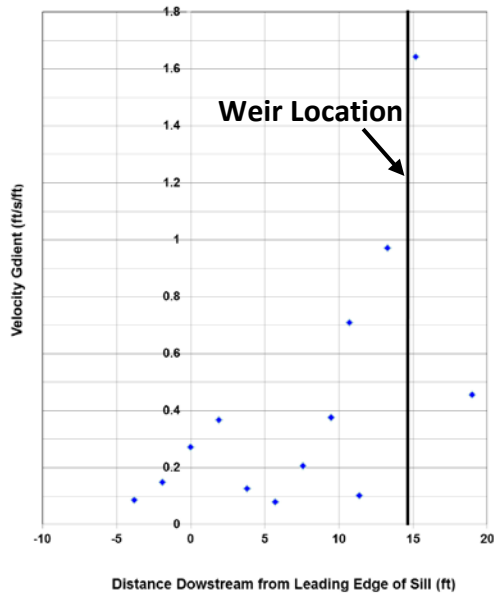


Figure C-14. — Velocity gradient measured 2 ft below the water surface approaching the 0.0 ft weir, operating at 400 ft<sup>3</sup>/s with a weir depth of 4.45 ft.

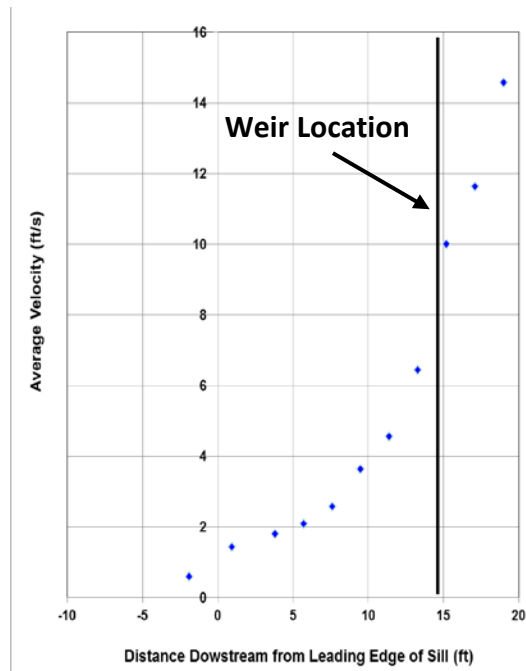


Figure C-15. — Average velocity measured 2 ft below the water surface approaching the 0.0 ft weir, operating at 200 ft<sup>3</sup>/s with a weir depth of 2.87 ft.

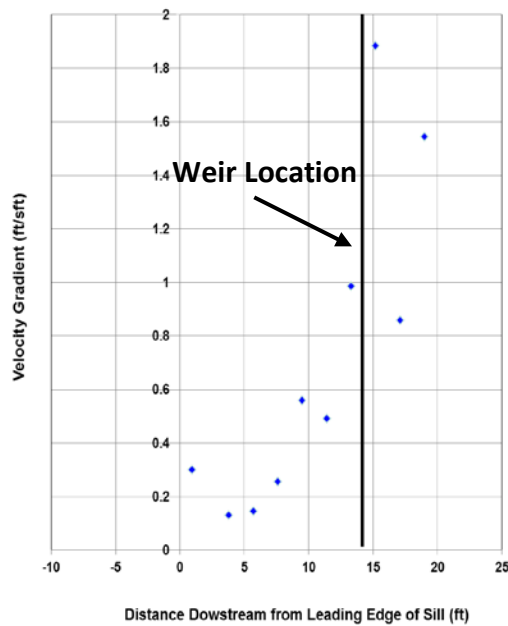


Figure C-16. — Velocity gradient measured 2 ft below the water surface approaching the 0.0 ft weir, operating at 200 ft<sup>3</sup>/s with a weir depth of 2.87 ft.

### Ramp-Weir Tests

An upstream ramp was added to each weir configuration to create a structure described as a ramp-weir. The ramps were extended from the upstream edge of

the inlet sill to the upstream edge of the weir for weir heights of 5.5 ft and 2.375 ft (Figure C-17 and Figure C-18). Both configurations were tested with flow rates of 200 ft<sup>3</sup>/s and 400 ft<sup>3</sup>/s. Velocity and velocity gradients measured 2 ft below the water surface for each test case are plotted in Figure C-19 through C-26. For each test case, capture velocity was reached as flow passed over the ramp-weir crest or just prior to going over the crest. For each of these tests, velocity gradient rose at a more gradual rate than with the weir alone, so that the gradient of 0.2 ft/s/ft was exceeded 5-10 ft upstream from the crest. The original criteria of 1.0 ft/s/ft was never exceeded before going over the crest of the 5.5 ft ramp-weir and was exceeded 2-3 ft upstream from the crest of the 2.375 ft ramp-weir.

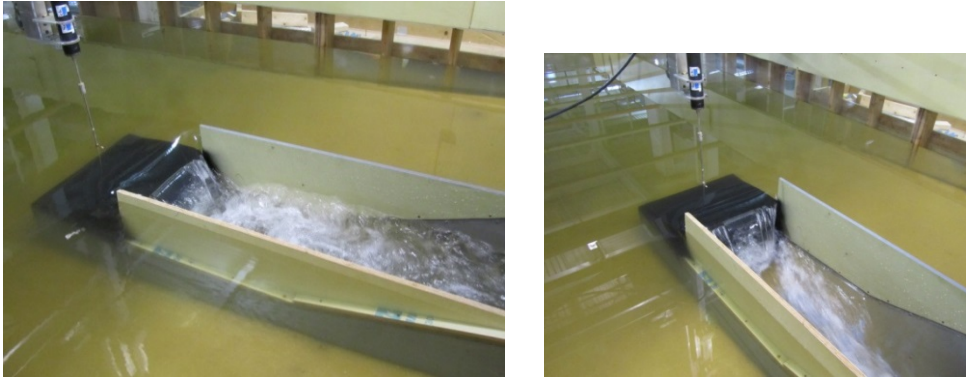


Figure C-17. — Ramp-weir height 5.5 ft operating at 400 ft<sup>3</sup>/s (left) and 200 ft<sup>3</sup>/s (right) with depth over the crest at 3.91 ft and 2.42 ft respectively

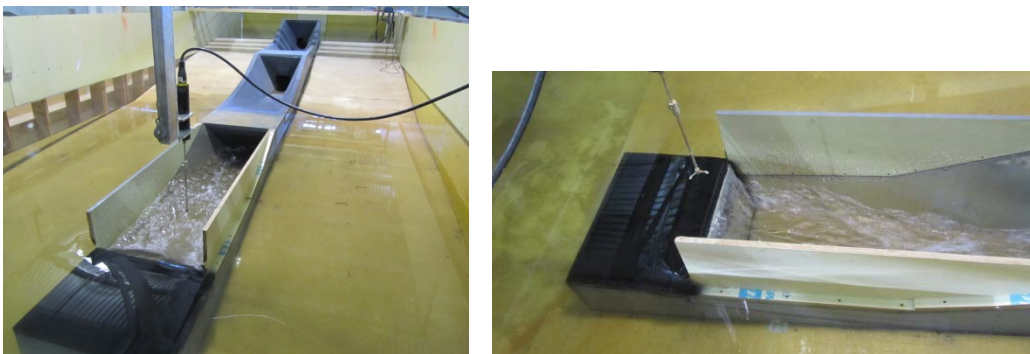


Figure C-18. — Ramp-weir height 2.375 ft operating at 400 ft<sup>3</sup>/s (left) and 200 ft<sup>3</sup>/s (right) with depth over the crest at 4.05 ft and 2.57 ft respectively.

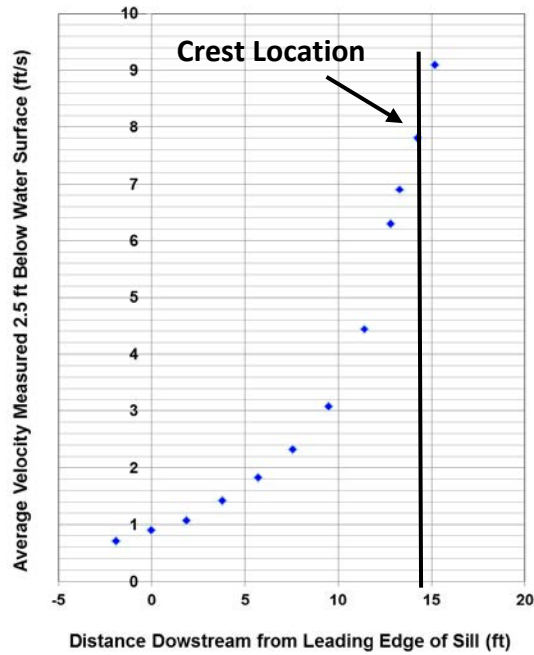


Figure C-19. — Average velocity measured 2 ft below the water surface approaching the 5.5 ft ramp-weir, operating at 400 ft<sup>3</sup>/s with a crest depth of 3.91 ft.

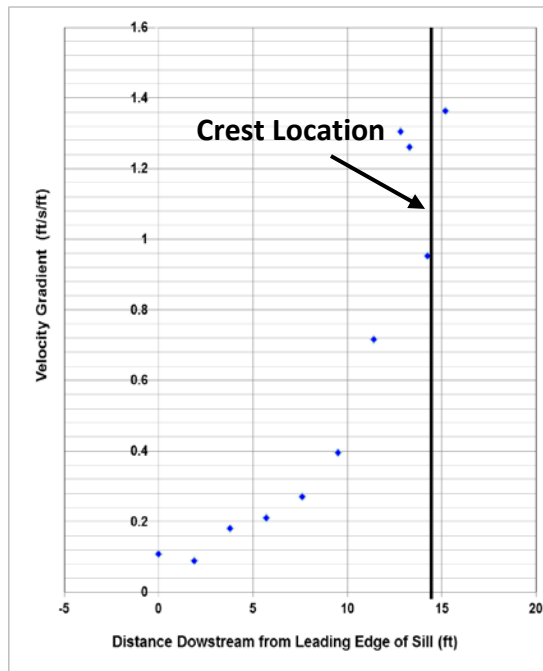


Figure C-20. — Velocity gradient measured 2 ft below the water surface approaching the 5.5 ft ramp-weir, operating at 400 ft<sup>3</sup>/s with a crest depth of 3.91 ft.

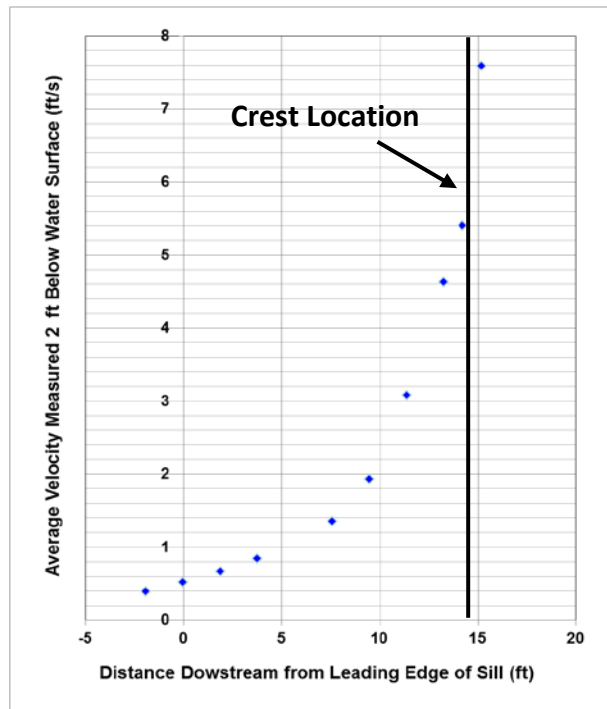


Figure C-21. — Average velocity measured 2 ft below the water surface approaching the 5.5 ft ramp-weir, operating at 200 ft<sup>3</sup>/s with a crest depth of 2.42 ft.

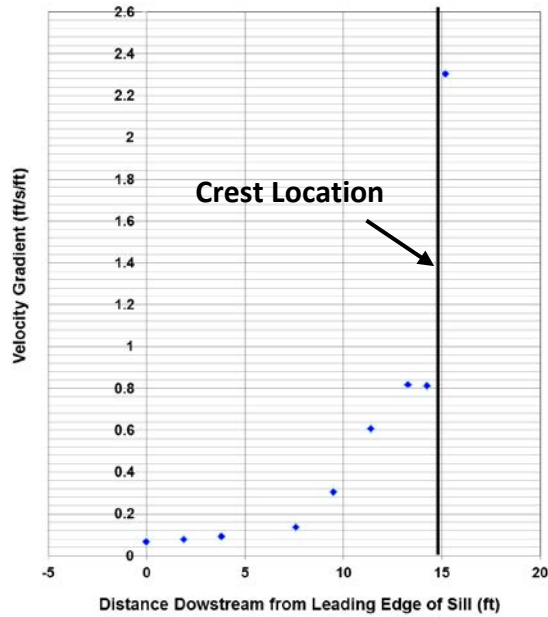


Figure C-22. — Velocity gradient measured 2 ft below the water surface approaching the 5.5 ft ramp-weir, operating at 200 ft<sup>3</sup>/s with a crest depth of 2.42 ft.

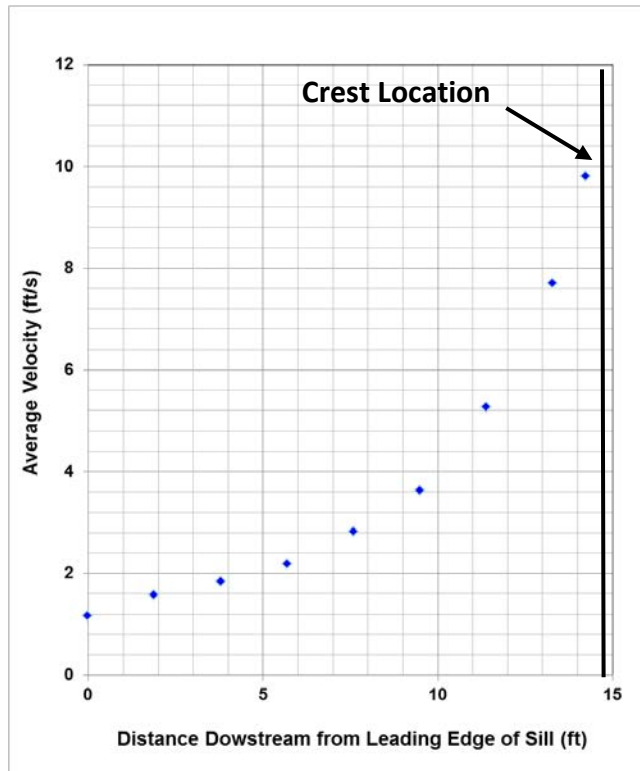


Figure C-23. — Average velocity measured 2 ft below the water surface approaching the 2.375 ft ramp-weir, operating at 400 ft<sup>3</sup>/s with a crest depth of 4.05 ft.

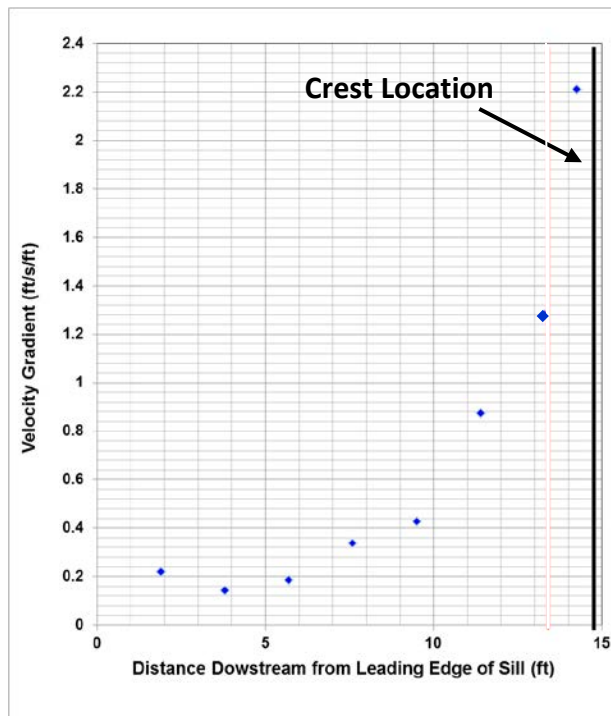


Figure C-24. — Velocity gradient measured 2 ft below the water surface approaching the 2.375 ft ramp-weir, operating at 400 ft<sup>3</sup>/s with a crest depth of 4.05 ft.

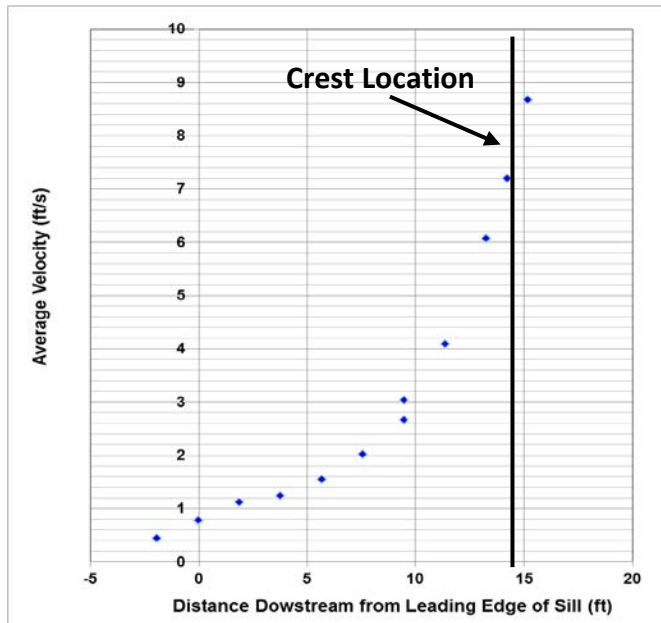


Figure C-25. — Average velocity measured 2 ft below the water surface approaching the 2.375 ft ramp-weir, operating at 200 ft<sup>3</sup>/s with a crest depth of 2.57 ft.

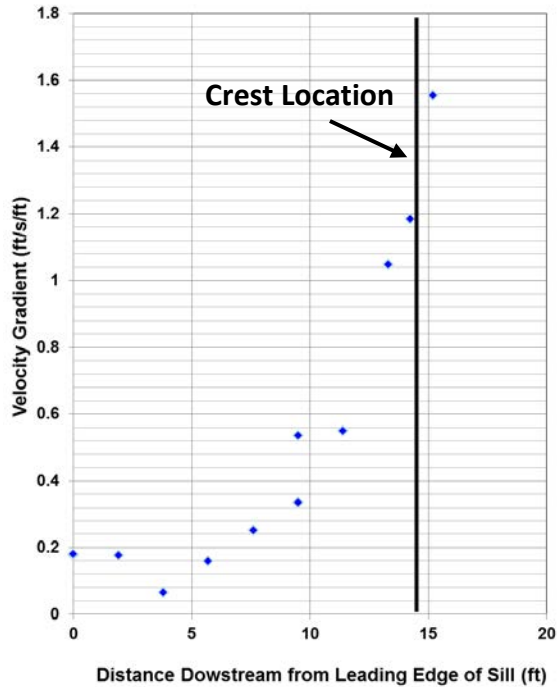


Figure C-26. — Velocity gradient measured 2 ft below the water surface approaching the 2.375 ft ramp-weir, operating at 200 ft<sup>3</sup>/s with a crest depth of 2.57 ft.